

Dynamics and bifurcations of a family of piecewise smooth maps arising in population models with threshold harvesting

Cite as: Chaos 30, 073108 (2020); <https://doi.org/10.1063/5.0010144>

Submitted: 08 April 2020 . Accepted: 17 June 2020 . Published Online: 06 July 2020

Eduardo Liz , and Cristina Lois-Prados 



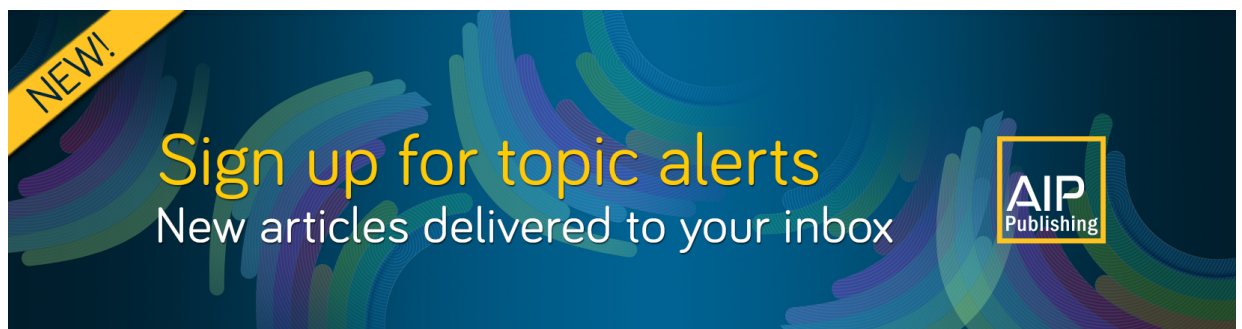
View Online



Export Citation



CrossMark



NEW!

Sign up for topic alerts
New articles delivered to your inbox

AIP
Publishing



Dynamics and bifurcations of a family of piecewise smooth maps arising in population models with threshold harvesting

Cite as: Chaos 30, 073108 (2020); doi: 10.1063/5.0010144

Submitted: 8 April 2020 · Accepted: 17 June 2020 ·

Published Online: 6 July 2020



View Online



Export Citation



CrossMark

Eduardo Liz^{1,a)}  and Cristina Lois-Prados^{2,b)} 

AFFILIATIONS

¹Departamento de Matemática Aplicada II, Universidade de Vigo, 36310 Vigo, Spain

²Instituto de Matemáticas, Universidade de Santiago de Compostela, Campus Vida, 15782 Santiago de Compostela, Spain

^{a)}Author to whom correspondence should be addressed: eliz@dma.uvigo.es

^{b)}Electronic mail: cristina.lois.prados@usc.es

ABSTRACT

We study a discrete-time model for a population subject to harvesting. A maximum annual catch H is fixed, but a minimum biomass level T must remain after harvesting. This leads to a mathematical model governed by a continuous piecewise smooth map, whose dynamics depend on two relevant parameters H and T . We combine analytical and numerical results to provide a comprehensive overview of the dynamics with special attention to discontinuity-induced (border-collision) bifurcations. We also discuss our findings in the context of harvest control rules.

Published under license by AIP Publishing. <https://doi.org/10.1063/5.0010144>

In the context of sustainable exploitation of natural resources (fishing, forestry, hunting), it is crucial to reduce the exploitation rate at low stock size. Harvest policies aiming at protecting endangered species are based on reference points such as a maximum allowable catch or a minimum biomass level that must remain after harvesting. Discrete-time mathematical models for these harvesting strategies lead in a natural way to piecewise smooth maps, whose dynamics are challenging because multiple discontinuity-induced bifurcations may appear. In this paper, we provide a thorough analysis of a threshold harvesting model depending on two parameters: a maximum harvesting quota and a minimum population threshold with a twofold aim of understanding the interplay between both parameters and uncovering interesting features of the underlying piecewise smooth map.

I. INTRODUCTION

In the context of chaos control, some strategies based on thresholding or limiter controls have been proposed to stabilize a fixed point or a desired periodic orbit.^{8,15,32} The same mechanism determines effective harvest control rules to prevent population collapses in fisheries and forestry.^{10,26}

A simple threshold mechanism to control a variable x is the following: choose a critical threshold T in such a way that whenever the value of x exceeds T , it is reset to T .³³ In the framework of sustainable harvesting, the same mechanism is known as threshold harvesting (TH); this harvest control rule removes the surplus of a population above a given threshold T (minimum biomass level) and takes no harvest below T . The recent paper (Ref. 18) includes a table collecting the many names of TH in different contexts.

When TH is applied to a one-dimensional map f , the controlled system is governed by a flat-topped map F . The dynamics of F is usually much simpler than the one of f , although it still has their own and interesting features (see, e.g., Refs. 32, 36, and 39). In particular, F is a non-smooth map, so some bifurcations different from the usual ones for smooth maps arise: the so-called border-collision bifurcations.²

Perhaps, the more relevant property for usual flat-topped maps is that almost all solutions converge to a periodic orbit containing T . Though this behavior can be seen as a nice property from a chaos control point of view, if TH is used as a harvesting rule, it opens the possibility of harvesting moratoria, with serious socioeconomic consequences. In the opposite side, a strategy of constant catch harvesting keeps the yield constant, rather than the escapement (biomass level after harvesting). It is well known that a serious drawback of

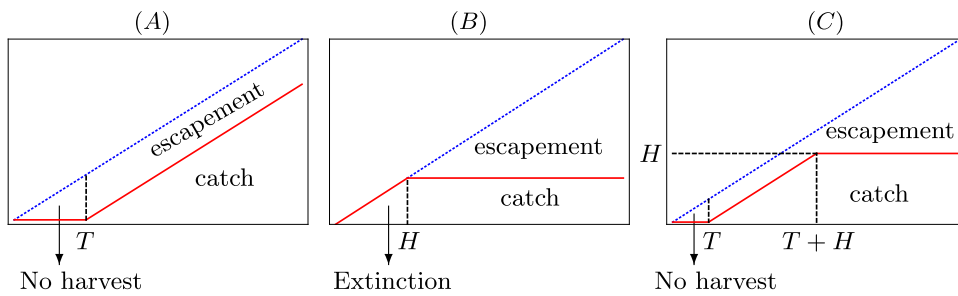


FIG. 1. Different harvesting strategies illustrated by sketching catch (red solid lines) as a function of population density or biomass. (a) Threshold harvesting, (b) constant quota harvesting, and (c) precautionary threshold constant-catch harvesting. The blue dotted lines indicate the identity diagonal line, T is the minimum biomass level, and H is the maximum allowed catch.

this method is that it highly elevates the risk of extinction, even leading to sudden collapses.^{26,30} Several combinations of the traditional harvesting strategies with protection rules based on thresholds have been proposed in order to minimize its drawbacks.^{10,12,13,17,26} In particular, a combination of threshold management and constant-catch harvesting was proposed by several authors.^{6,26,35} In the latter reference, this strategy was named “conditional fixed harvest.” The idea is simple: if population size is below a given threshold T , then no harvest is allowed; otherwise, we allow to catch a constant quota H but always ensuring that at least a minimum population stock T will remain after harvesting. Thus, there are two reference breakpoints: the maximum allowed catch H and the minimum biomass level T . In the spirit of Ref. 12, this harvesting rule can be seen as a precautionary modification of threshold constant-catch harvesting, and then we will refer to it as *precautionary threshold constant-catch harvesting* (PTCH for short). Figure 1 shows an illustration of the three mentioned harvesting policies: threshold harvesting, constant quota, and precautionary threshold constant-catch harvesting.

Our aim in this paper is twofold: first, we combine analytical and numerical results to provide a rigorous mathematical analysis of PTCH using a discrete-time single-species model; second, we show that our model is a simple but insightful example of piecewise smooth dynamical system, complementing in this way the growing set of applications of this class of dynamical systems.² As far as we know, we formulate and study this harvesting rule in the framework of dynamical systems for the first time. Our study is focused on stability and bifurcations; in this regard, we consider the two relevant harvest parameters T and H and obtain 1-parameter and 2-parameter bifurcation diagrams that help one to understand how a continuous variation of any of them influence the dynamics, and the interplay between both parameters. We identify regions where global attraction, periodic attractors, bistability, or complex behavior are likely to occur, paying special attention at border-collision bifurcations.

We organize the paper as follows: in Sec. II, we introduce the piecewise smooth one-dimensional map governing PTCH and the main assumptions on the involved functions. Section III is devoted to the study of fixed points: in Subsection III A, we give the location of positive equilibria depending on the relevant parameters; Subsection III B is devoted to provide stability results for the positive fixed points. In simple cases, all solutions converge to an equilibrium and in the general case, there are stability switches and the global picture is more complicated; we give some general results for global stability and study in more detail in the Ricker map, which is a prototype for discrete population models, especially in the context

of fisheries;^{27,29,38} and finally, in Subsection III C, we describe all possible bifurcations of fixed points (smooth and border-collision bifurcations). In Sec. IV, we focus on a particular region of the parameter plane for which chaos and essential attraction can occur. The latter means that an equilibrium is not globally attracting, but solutions converge to it with probability one. In Sec. V, we address two case studies: a simple compensatory model, where only bifurcations of fixed points appear and an overcompensatory model that exhibits richer dynamics; in both cases, numerical bifurcation diagrams help one to understand the influence of the parameters. Finally, in Sec. VI, we discuss the obtained results in the framework of piecewise smooth dynamical systems (with special attention to those with maps containing flat branches) and in the framework of harvesting strategies.

II. THE MODEL AND BASIC ASSUMPTIONS

To carry out a theoretical study of the dynamics induced by PTCH, we assume that population growth in the absence of harvesting is governed by a one-dimensional difference equation

$$x_{n+1} = f(x_n), \tag{1}$$

where x_n is the population density at time step $n, n = 0, 1, 2, \dots$, starting at an initial value $x_0 > 0$. The map f is the production (or stock–recruitment curve), for which we assume typical conditions for single-species population models,

(A1) $f: [0, \infty) \rightarrow [0, \infty)$ is continuous, has a unique positive fixed point $K, f(x) > x$ for $x \in (0, K)$, and $0 < f(x) < x$ for $x > K$. Moreover, $f(0) = 0$ and there exists $\lim_{x \rightarrow \infty} f(x) < \infty$.

Most of the results will require additional conditions, which are summarized in the next hypothesis,

(A2) f is a C^2 map having at most one critical point $x_c \in (0, \infty)$ such that $f'(x) > 0$ for all $x \in (0, x_c)$ and $f'(x) < 0$ for all $x > x_c$. Moreover, $f''(x) < 0$ on $(0, x_c)$. If f has no critical points, then we consider $x_c = \infty$, and hence, f is increasing. If f has one critical point, we assume that $\lim_{x \rightarrow \infty} f(x) = 0$.

Sometimes, we will also assume that f is a C^3 map with negative Schwarzian derivative.

We recall that the Schwarzian derivative is defined by the expression

$$(Sf)(x) = \left(\frac{f'''(x)}{f'(x)} \right) - \frac{3}{2} \left(\frac{f''(x)}{f'(x)} \right)^2,$$

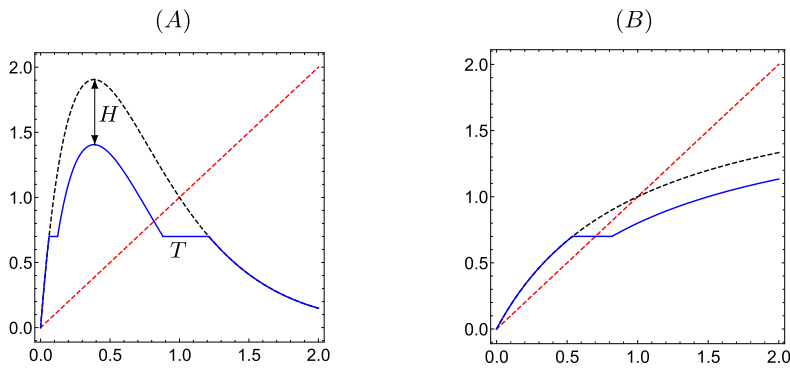


FIG. 2. Illustration of the graph of the piecewise smooth map F (blue solid line). We also plot the line $y = x$ (red, dashed) and the graph of f (black, dashed). (a) Unimodal Ricker map $f(x) = x e^{2.6(1-x)}$, with $H = 0.5$ and $T = 0.7$. (b) Monotone Beverton-Holt map $f(x) = 2x/(1+x)$, with $H = 0.2$ and $T = 0.7$.

whenever $f'(x) \neq 0$. When **(A2)** holds with finite x_c , the map f is unimodal; if, in addition, $(Sf)(x) < 0$ for all $x \neq x_c$, then f is an S -unimodal map.³⁸ The concavity condition on $(0, x_c)$ is not usually assumed for this type of maps, but it is not very restrictive: on the one hand, it is satisfied by the models we consider; on the other hand, for S -unimodal maps, $f''(0^+) < 0$ implies $f''(x) < 0$ for all $x \in (0, x_c)$.²¹

Both **(A1)** and **(A2)** hold for many compensatory and overcompensatory models usually employed in population dynamics. Throughout this paper, we understand that the model defined by (1) is *compensatory* if f satisfies **(A1)** and **(A2)** with $x_c \geq K$ (that is, f is nondecreasing at the positive equilibrium) and *overcompensatory* otherwise. For example, the compensatory Beverton-Holt model is defined by the map $f(x) = rx/(1+x)$, $r > 1$, which fulfills condition **(A1)** with $K = r - 1$, and condition **(A2)** with $x_c = \infty$. The Ricker model defined by $f(x) = x e^{r(1-x)}$, $r > 0$, satisfies **(A1)** with $K = 1$ and **(A2)** with $x_c = 1/r$. It is compensatory if $r \leq 1$ and overcompensatory if $r > 1$.

Applying the precautionary threshold constant-catch harvesting rule to (1) and assuming that populations are measured after reproduction and before harvesting, we obtain the difference equation

$$x_{n+1} = F(x_n) := \begin{cases} f(x_n) & \text{if } f(x_n) \leq T, \\ T & \text{if } T < f(x_n) \leq T + H, \\ f(x_n) - H & \text{if } f(x_n) > T + H. \end{cases} \quad (2)$$

For convenience, we define the map $g(x) = f(x) - H$, which allows us to write F in the form

$$F(x) = \begin{cases} f(x) & \text{if } f(x) \leq T, \\ T & \text{if } g(x) \leq T < f(x), \\ g(x) & \text{if } T < g(x). \end{cases}$$

The piecewise smooth continuous map F can also be written in a line as

$$F(x) = \min \{ f(x), f(x) - \min\{H, f(x) - T\} \} \\ = \min \{ f(x), \max\{g(x), T\} \}$$

and depends on the two harvesting parameters H and T . The typical shape of F can be seen in Fig. 2. Roughly speaking, the graphs of f and g are joined by flat segments defined by T , which typically results in

five intervals of smoothness for F if f is unimodal and three if f is nondecreasing.

Throughout the paper, we will assume that $H > 0$ and $T > 0$. It is clear that $F \equiv f$ if $H = 0$ or $T \geq \sup\{f(x), x \geq 0\}$. In the limit case $T = 0$, (2) becomes the usual constant catch policy, defined by the map $F(x) = \max\{f(x) - H, 0\}$.

It is also worth noticing that if $T < \sup\{f(x), x \geq 0\} \leq H + T$, then the precautionary threshold constant-catch harvesting strategy (PTCH) becomes the pure threshold harvesting rule (TH), defined by the map $F(x) = \min\{f(x), T\}$ (see Ref. 18).

For convenience of the readers, we include some important notations in Table I. Some of them have been already introduced, and others will appear in the following.

TABLE I. Main notations.

Symbol/concept	Meaning
H	(Maximum) harvesting quota
T	Threshold harvesting parameter
PTCH	Precautionary threshold constant-catch harvesting
TH	(Pure) threshold harvesting
f	Production map governing (1)
g	$g(x) = f(x) - H$
F	Map defining the PTCH rule (2)
Ricker map	$f(x) = x e^{r(1-x)}$, $r > 0$
x_c	Critical point of f ($f'(x_c) = 0$)
\tilde{x}	Point such that $f'(\tilde{x}) = 1$
\bar{x}	(Smallest) point such that $f'(\bar{x}) = -1$
K	Positive fixed point of f
p, q	Positive fixed points of g ($0 < p \leq q < K$)
break point	Point at which F is not differentiable
boundary fixed point	Break point which is a fixed point of F
admissible fixed point	Fixed point of F
virtual fixed point	Fixed point of one map defining F but not of F
BCB	Border-collision bifurcation
SB	Smooth bifurcation

III. FIXED POINTS: LOCATION, STABILITY, AND BIFURCATIONS

In this section, we study the fixed points of F depending on the parameter values T and H . In the first subsection, we focus on the number of fixed points and their location; in the second one, we study their stability properties; and in the third subsection, we describe the local bifurcations of fixed points, that is, we determine the critical values of the parameters for which fixed points are created or destroyed, or stability switches occur.

One important consequence of conditions (A1) and (A2) is that there is a unique $\tilde{x} > 0$ such that $f'(\tilde{x}) = 1$. Moreover, $\tilde{x} \in (0, \min\{K, x_c\})$. This property is a direct consequence of the mean value theorem, and the concavity of f on $(0, x_c)$. The point \tilde{x} plays an important role in the study of fixed points.

A. Positive fixed points

The following result provides the number of positive fixed points of the map F defined in (2). Notice that 0 is a fixed point of F , and it is always unstable. We assume that $T > 0$ and $H > 0$.

Proposition 1: Assume that (A1) and (A2) hold and denote by \tilde{x} the unique solution of $f'(x) = 1$. Then,

- (i) If $T \geq K$, then K is the unique positive equilibrium of (2).
- (ii) If $\tilde{x} \leq T < K$, then F has a unique positive fixed point, which is T if $H \geq f(T) - T$, and a fixed point $q \in (T, K)$ of g if $H < f(T) - T$.
- (iii) If $0 < T < \tilde{x}$, then
 - (a) F has a unique positive fixed point $q \in (\tilde{x}, K)$ if $H < f(T) - T$.
 - (b) F has three positive fixed points (T and two fixed points of g) if $f(T) - T < H < f(\tilde{x}) - \tilde{x}$.
 - (c) T is the unique positive fixed point of F if $H > f(\tilde{x}) - \tilde{x}$.
 - (d) F has two positive fixed points if either $H = f(T) - T$ or $H = f(\tilde{x}) - \tilde{x}$.

Proof. In view of (2), K is a fixed point of F if and only if $K = f(K) \leq T$. Moreover, if $K \leq T$, then K is the only positive fixed point of F because $F(x) \geq \min\{f(x), T\} > x$ if $x < K$, and $F(x) \leq f(x) < x$ if $x > K$.

If $T < K$, then there are two possibilities for the positive fixed points of F : the threshold T and the positive equilibria of g .

It is obvious from the definition of F that T is a fixed point if and only if $f(T) \leq T + H$, that is, $H \geq f(T) - T$.

Since $g'(x) = f'(x)$ and $g''(x) = f''(x)$, g can have at most two positive fixed points. Assume that $p < q$ are two fixed points of g . Then, by the mean value theorem, $p < \tilde{x} < q$, where \tilde{x} is the only point for which $f'(\tilde{x}) = 1$. It also follows that $T < p < q < K$ because $p = F(p) = g(p) = f(p) - H > T$ and $g(x) = f(x) - H \leq x - H < x$ for all $x \geq K$.

Now, statements (ii) and (iii) follow easily. We include the proof of (ii) and leave the other to the reader.

Assume $\tilde{x} \leq T < K$. If $H \geq f(T) - T$, then T is a fixed point of F , and it is the only one because $g(T) \leq T$ and $g(x) < 1$ for all $x > T$.

If $H < f(T) - T$, then F has a fixed point $q \in (T, K)$ because $g(T) = f(T) - H > T$ and $g(K) = f(K) - H = K - H < K$. This

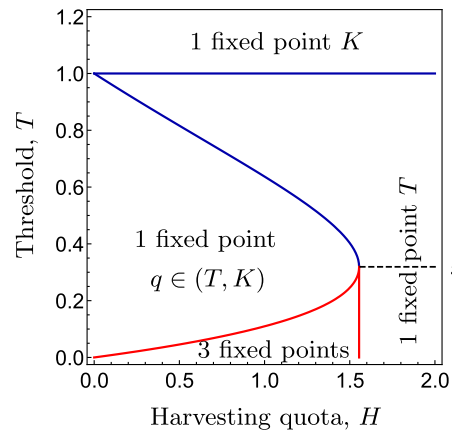


FIG. 3. Number of positive fixed points of F with the Ricker map $f(x) = x e^{2.6(1-x)}$. There are two positive fixed points for the parameter values in the boundaries colored in red: $H = f(T) - T$, $0 < T < \tilde{x}$ and $H = f(\tilde{x}) - \tilde{x}$, $0 < T < \tilde{x}$. There is only one positive fixed point for parameters at the boundaries colored in blue: $H = f(T) - T$, $\tilde{x} < T < 1$ and $T = 1$.

fixed point is unique because if there were two fixed points $p < q$, then $T < p$ and $g(x) < x$ for all $x < p$ would imply that $g(T) < T$, a contradiction. \square

Figure 3 illustrates the number of fixed points in the parameter plane (H, T) .

B. Stability of fixed points

This section is devoted to study the stability properties of the positive fixed points of F . We divide it into three parts: first, we deal with compensatory models; then, we give some global stability results; finally, we focus on the Ricker model. The points K , \tilde{x} , and x_c have the same meaning as in Sec. III A (see Table I).

As usual, we say that a fixed point x^* of a map $h : I \rightarrow I$ is stable if for each neighborhood V of x^* in I there exists a neighborhood U of x^* in I such that $h^n(x) \in V$ for all $x \in U$ and all $n \geq 1$. x^* is (locally) asymptotically stable (LAS for short) if it is stable and is a local attractor, that is, there exists an interval J containing x^* such that $\lim_{n \rightarrow \infty} h^n(x) = x^*$ for all $x \in J$. If $J = I$, we say that x^* is a global attractor (or globally attracting). Since globally attracting fixed points of continuous interval maps must be stable, a global attractor is sometimes called globally asymptotically stable (GAS for short). Finally, we say that x^* is semistable if it is not stable but attracts either $[x^*, x^* + \varepsilon)$ or $(x^* - \varepsilon, x^*]$, for some $\varepsilon > 0$.

We recall that, by Singer's results,³⁴ if f is an S-unimodal map with a unique fixed point x^* , then x^* is a global attractor if $f'(x^*) \geq -1$, and unstable if $f'(x^*) < -1$. We will use the following more general result (Ref. 11, Corollary 2.9):

Lemma 1: Let $g : I \rightarrow Cl(I)$ be a continuous function with a unique fixed point x^* such that $g(x) > x$ if $x < x^*$, and $g(x) < x$ if $x > x^*$. [Here, I is a real interval and $Cl(I)$ denotes its closure.] Assume that there are points $c, d \in I$ such that $c < x^* < d$ and the restriction of g to (c, d) has at most one turning point and (whenever it makes sense) $g(x) \leq g(c)$ for every $x \leq c$ and $g(x) \geq g(d)$

for every $x \geq d$. If g is decreasing at x^* , assume additionally that $(Sg)(x) < 0$ for all $x \in (c, d)$ except at most one critical point of g and $-1 \leq g'(x^*) < 0$. Then, x^* is a global attractor of g .

The following technical result will be also useful. It is a simple generalization of Ref. 4, Lemma 1.

Lemma 2: Let $f: (a, b) \rightarrow (a, b)$ be a continuous function defined on a real interval (a, b) ($-\infty \leq a < b \leq \infty$) such that f has a unique fixed point x^* with $x < f(x) < x^*$ for all $x \in (a, x^*)$ and $a < f(x) < x$ for all $x \in (x^*, b)$. Then, x^* is a global attractor of f .

1. Compensatory models

Compensatory models exhibit simple dynamics. Recall that the model defined by (1) is compensatory if f satisfies (A1) and (A2) with $x_c \geq K$. This framework includes monotone maps like in the Beverton–Holt model, and unimodal maps as the Ricker function $f(x) = xe^{r(1-x)}$ with $0 < r \leq 1$. Lemma 2 ensures that for compensatory models, K is a global attractor of the model without harvesting (1).

For the model with harvesting, we get the following result:

Theorem 1: Assume that f satisfies (A1) and (A2) with $T < K \leq x_c$. Then, every solution of (2) converges to an equilibrium. More specifically,

- (a) If $H < f(T) - T$, then there is a unique positive equilibrium $q \in (T, K)$ of F and it is globally attracting.
- (b) If $H \geq f(T) - T$ and $T \geq \tilde{x}$, or $T < \tilde{x}$ and $H > f(\tilde{x}) - \tilde{x}$, then T is the unique positive equilibrium of F and it is globally attracting.
- (c) If $f(T) - T \leq H \leq f(\tilde{x}) - \tilde{x}$, then there is bistability between two positive equilibria: T and $q \in (T, K)$. If $H < f(\tilde{x}) - \tilde{x}$, denote by p the largest fixed point of F smaller than q , and $p^* = \min\{x \in F^{-1}(\{p\}) : x > p\}$ [$p^* = \infty$ if there are no $x > p$ such that $F(x) = p$]. If $f(T) - T < H < f(\tilde{x}) - \tilde{x}$, then the basin of attraction of T is $(0, p) \cup (p^*, \infty)$ and the basin of attraction of q is (p, p^*) . If $H = f(\tilde{x}) - \tilde{x}$, then $q = p$ is semistable and its basin of attraction is $[p, p^*]$. If $H = f(T) - T$, then $T = p$ and the basin of attraction of T is $(0, p) \cup [p^*, \infty)$.

Proof. The proofs of (a) and (b) follow from Lemma 2. Next, we prove (c) when $f(T) - T < H < f(\tilde{x}) - \tilde{x}$. On the one hand, F maps the interval $I = (p, p^*)$ into itself, and Lemma 2 ensures that q attracts I . On the other hand, F maps the interval $J = (0, p)$ into itself, and Lemma 2 also applies to prove that T attracts J . Finally, it is clear that F maps (p^*, ∞) on J . The limit cases $H = f(\tilde{x}) - \tilde{x}$ and $H = f(T) - T$ are left to the reader. \square

If $T \geq K$, then the equilibrium K is a global attractor (see Theorem 2 below).

2. Global stability results

In this subsection, we provide some sufficient conditions under which the positive equilibrium is unique and globally attracting.

The first case occurs when $T \geq K$, which is considered in the next result. The proof is shifted to Appendix A 1.

Theorem 2: Assume that f satisfies (A1) and K is a global attractor of f . If $T \geq K$, then K is a global attractor of F .

In the following, we assume that (A1) and (A2) hold. Our next result deals with sufficient conditions for the global stability of T when $T < K$. Since the compensatory case was studied in Subsection III B 1, we deal with the overcompensatory case.

Theorem 3: Assume that $T < K$ and $H \geq f(T) - T$. If any of the following conditions holds, then T is the unique positive fixed point of F , and it is globally asymptotically stable.

- (a) $T < \tilde{x}$ and $H > f(\tilde{x}) - \tilde{x}$;
- (b) $\tilde{x} \leq T \leq x_c$;
- (c) $f(x_c) - H \leq T < K$; and
- (d) $f(g(x_c)) \geq T$ and $T > x_c$.

Proof. In all cases, it follows from Proposition 1 that T is the unique positive fixed point of F . In cases (a) and (b), it is easy to check that $x < F(x) \leq T$ for $x < T$ and $0 < F(x) < x$ for $x > T$. Hence, the result follows from Lemma 2.

Since scheme (2) becomes threshold harvesting when $H + T \geq f(x_c)$, in case (c), the result follows from Ref. 18, Proposition 2.1. Finally, conditions in (d) imply that the long-term behavior of the solutions of (2) and equation $x_{n+1} = G(x_n)$, $n \geq 0$, is the same, where

$$G(x) = \begin{cases} T & \text{if } g(x) \leq T, \\ g(x) & \text{if } g(x) > T. \end{cases} \quad (3)$$

Since T is stable for G , to prove the global stability it is enough to exclude periodic orbits of G with prime period 2 (see, e.g., Ref. 14, Proposition 1). But G cannot have 2-periodic orbits because $G(x) = T$ for all $x \geq T$. \square

In line with case (d) in the previous theorem, we can prove a global stability result for the fixed point q in case f is S -unimodal.

Theorem 4: Assume that $T < K$, $H < f(T) - T$, and f is S -unimodal. If $g'(q) \geq -1$ and $f(g(x_c)) \geq T$, then q is globally asymptotically stable.

Proof. Condition $H < f(T) - T$ implies that q is the unique positive fixed point of F . Since $f(g(x_c)) \geq T$, F can be replaced by map G defined in (3) for the analysis of convergence of solutions, as in the proof of Theorem 3. Now, the proof easily follows from Lemma 1, with $c = \min g^{-1}(T)$ and $d = \max g^{-1}(T)$. \square

We illustrate the results of Theorems 3 and 4 in Fig. 4.

3. Specific results for the Ricker map

In this subsection, we focus our attention on the PTCH scheme (2) with the Ricker map $f(x) = xe^{r(1-x)}$, $r > 1$, in order to give a more comprehensive description of the stability properties of the positive equilibria. Recall that the case $r \leq 1$ has been addressed in Subsection III B 1.

We recall some basic properties of the Ricker map. First, f is an S -unimodal map. In particular, f fulfills (A1) and (A2) with $K = 1$ and $x_c = 1/r$, and there exists a unique $\tilde{x} \in (0, 1/r) \subset (0, 1)$ such that $f'(\tilde{x}) = 1$.

Since $f'(x) = (1 - rx)e^{r(1-x)}$ and $f''(x) = -r(2 - rx)e^{r(1-x)}$, it follows that $f''(x) < 0$ for all $x \in (0, 2/r)$, $f''(2/r) = 0$ and $f''(x) > 0$ for all $x > 2/r$. Hence, f' attains its global minimum at $2/r$ and $f'(2/r) = -e^{r-2} < -1$ if and only if $r > 2$. Thus, since f is an S -unimodal map, we have the following known result, which we state for later reference.

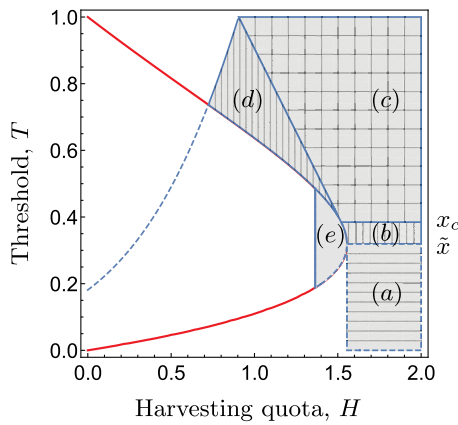


FIG. 4. Regions of global stability for PTCH with the Ricker map $f(x) = xe^{2.6(1-x)}$ based on Theorems 3 and 4. The red solid curve is the graph of $H = f(T) - T$. T is GAS in regions defined by $H > f(T) - T$ and (a) $T < \bar{x}$ and $H > f(\bar{x}) - \bar{x}$; (b) $\bar{x} \leq T \leq x_c$, (c) $f(x_c) - H \leq T < K$; and (d) $f(g(x_c)) \geq T$ and $T > x_c$. Notice that when $H < f(T) - T$, condition $f(g(x_c)) \geq T$ holds to the right of the dashed line, so q is globally stable in region (e), determined by condition $g'(q) \geq -1$ (see Theorem 7).

Proposition 2: If $f(x) = xe^{r(1-x)}$ and $0 < r \leq 2$, then $f'(x) \geq -1$ for all $x > 0$. Moreover, $f'(x) = -1$ if and only if $r = 2$ and $x = 1$. In particular, if $r \leq 2$, then the positive equilibrium $K = 1$ is a global attractor of f in $(0, \infty)$. If $r > 2$, then $f'(K) = 1 - r < -1$, and, therefore, K is unstable.

If $r > 2$, then there exists a unique $\bar{x} \in (x_c, 2/r)$ such that $f'(x) \in (-1, 0)$ for all $x \in (x_c, \bar{x})$, $f'(\bar{x}) = -1$, and $f'(x) < -1$ for all $x \in (\bar{x}, 1)$. The value of \bar{x} can be numerically computed as the smallest root of equation $f'(x) = -1$, that is, the unique solution $x \in (0, 1)$ of $(rx - 1)e^{r(1-x)} = 1$.

We begin considering the case when the Ricker map has a stable equilibrium. The proofs of Theorems 5 and 6 are provided in Appendix A 2. They consider the cases when F has at least one positive fixed point different from T , or T is the unique positive fixed point of F , respectively.

Theorem 5: Assume $1 < r \leq 2$, $T < 1$, and F has at least one positive fixed point different from T . Denote by p, q ($p \leq q$) the positive fixed points of g . Then, there are two possibilities:

- (i) If T is a fixed point of F (that is, $H \geq f(T) - T$), then there are three cases. If there are three positive fixed points of F ($T < p < q$), then q attracts (p, p^*) and T attracts $(0, p) \cup (p^*, \infty)$, where $p^* = \max g^{-1}(p)$. If there are two positive fixed points of F ($T = p < q$), then q attracts (T, T^*) and T attracts $(0, T] \cup [T^*, \infty)$, where $T^* = \min\{x > T : g(x) = T\}$. If there are two positive fixed points of F ($T < p = q$), then q attracts $[p, p^*]$ and T attracts $(0, p) \cup (p^*, \infty)$.
- (ii) If $H < f(T) - T$, then q is the unique positive fixed point of F , and it is a global attractor.

Theorem 6: If $1 < r \leq 2$, $x_c < T < 1$ and $H \geq f(T) - T$, then T is the unique positive fixed point of F , and it is globally asymptotically stable.

Now, we are in a position to state and prove the main result in this subsection.

Theorem 7: Consider the map F defined by (2) with $f(x) = xe^{r(1-x)}$, $r > 1$. Denote by p, q , the fixed points of $g(x) = f(x) - H$, when they exist, with $T < p \leq q$.

- (I) If $T \geq 1$, then the positive fixed point $K = 1$ of f is the unique positive equilibrium of F . It is a global attractor if $1 < r \leq 2$ and unstable if $r > 2$.
- (II) If $T < 1$ and $1 < r \leq 2$, then the conclusions (a), (b), and (c) of Theorem 1 hold. In particular, every solution of (2) with initial condition $x_0 > 0$ converges to a positive equilibrium.
- (III) If $T < 1$ and $r > 2$, then,
 - T is a fixed point of F if and only if $H \geq f(T) - T$ and $T \leq 1$. Moreover, T is semi-stable if $0 < T < \bar{x}$ and $H = f(T) - T$, and it is asymptotically stable otherwise. T is a global attractor in the cases stated in Theorem 3 (see Fig. 4).
 - The fixed point p is unstable if $p < q$, and semi-stable if $p = q$.
 - The fixed point $q \in (\bar{x}, 1)$ is unstable if $H < f(\bar{x}) - \bar{x}$, and asymptotically stable if $H \geq f(\bar{x}) - \bar{x}$. In the latter case, q is a global attractor if $f(g(x_c)) \geq T$.

Proof. The existence of the different fixed points of F is given in Proposition 1. The proof of (I) follows from Theorem 2 and Proposition 2. The proof of (II) follows from Theorems 3, 5, and 6.

Next, we consider the three cases of (III):

- First, we deal with the stability of the threshold value T . If $H > f(T) - T$, then T is asymptotically stable because F is differentiable in an interval $(T - \varepsilon, T + \varepsilon)$, and $f'(T) = 0$. When $H = f(T) - T$, we distinguish several cases: First, if $T > x_c$, then there exists $m_1 > 0$ such that $F(x) = T$ for all $x \in [T, T + m_1)$, which, by continuity, implies that there exists $m_2 > 0$ such that $F^2(x) = T$ for all $x \in (T - m_2, T)$; therefore, T is asymptotically stable. Next, if $\bar{x} \leq T \leq x_c$, then T is the unique positive fixed point of F , and it is globally stable (see Theorem 3). When $T \in (0, \bar{x})$, T is semi-stable because there is $\eta > 0$ such that $F(x) = T$ for $x \in (T - \eta, T]$, and $F'(T^+) > 1$.
- As for the smallest fixed point of g , p is unstable if $p < q$ because $F(x) = g(x)$ in a neighborhood of p and $p < \bar{x}$. Hence, $F'(p) = f'(p) > 1$. When p and q collide, there is a smooth tangent bifurcation and p is semistable.
- Finally, we address the stability of $q \in (\bar{x}, 1)$. Since $F(x) = g(x)$ in a neighborhood of q , the asymptotic stability of q depends on $g'(q) = f'(q)$. Since $q \in (\bar{x}, K)$, it is clear that q is asymptotically stable if $q \leq \bar{x}$ (that is, $H \geq f(\bar{x}) - \bar{x}$), and unstable if $q > \bar{x}$ ($H < f(\bar{x}) - \bar{x}$). The global stability result follows from Theorem 4. □

C. Bifurcations of fixed points

The boundaries found in Subsection III A help us to analyze the possible bifurcations of fixed points, using the bifurcation parameters H and T . Since F is a piecewise smooth continuous map, some bifurcations are non-smooth. We adopt some notations in Ref. 2; see Table 1 for quick reference in the future.

The points where F is not differentiable are called *break points*. When a break point x^* is a fixed point of the map F , then we call

x^* a boundary fixed point. Boundary fixed points determine a kind of bifurcations that are called border-collision bifurcations since the work of Nusse and Yorke.²⁴ Border-collision bifurcations (BCB for short) occur when, under variation of some parameters, a fixed point or a cycle collides with a break point, and this collision leads to a qualitative change in the dynamics. Sometimes, we use the term *discontinuity-induced bifurcations* for other type of bifurcations in which a break point is involved (for example, when the metric attractor is an interval, and one of its endpoints collides with a break point). For usual bifurcations where break points are not involved, we use the term *smooth bifurcations* (SB for short). We emphasize that F is continuous, so discontinuity refers to its first derivative.

According to Ref. 2, Sec. 3.1.2, there are four basic possible dynamical scenarios at a BCB defined by a boundary fixed point. We need the notions of admissible and virtual fixed points. For the PTCH rule (2), we recall that F is a piecewise smooth map defined by three differentiable maps: f , g , and the constant function T . A fixed point of F is called an *admissible fixed point*, whereas a *virtual fixed point* is a fixed point of one of the smooth maps defining F but not a fixed point of F . For example, T and K are either virtual or admissible

fixed points of F ; according to Proposition 1, K is admissible if and only if $T \geq K$, and T is admissible if and only if $H \geq f(T) - T$ and $T \leq K$.

- A *fold BCB* occurs when two coexisting admissible fixed points collide at a break point and become two virtual fixed points.
- A *flip BCB* or *period-doubling BCB* occurs when an admissible fixed point collides with a break point and a 2-periodic orbit $\{p_1, p_2\}$ appears, where p_1 and p_2 are at different sides of the break point.
- A *persistence BCB* occurs when an admissible and a virtual fixed point collide at a break point and interchange their roles. No other periodic points are created or destroyed at the bifurcation point.
- A *period-multiplying BCB* occurs when an admissible fixed point collides with a break point and an m -periodic orbit appears, with $m > 2$.

In our framework, these bifurcations can only occur when T becomes a boundary fixed point, that is, when $g(T) = T$ [equivalently, $H = f(T) - T$] or $f(T) = T$ (equivalently, $T = K$). When

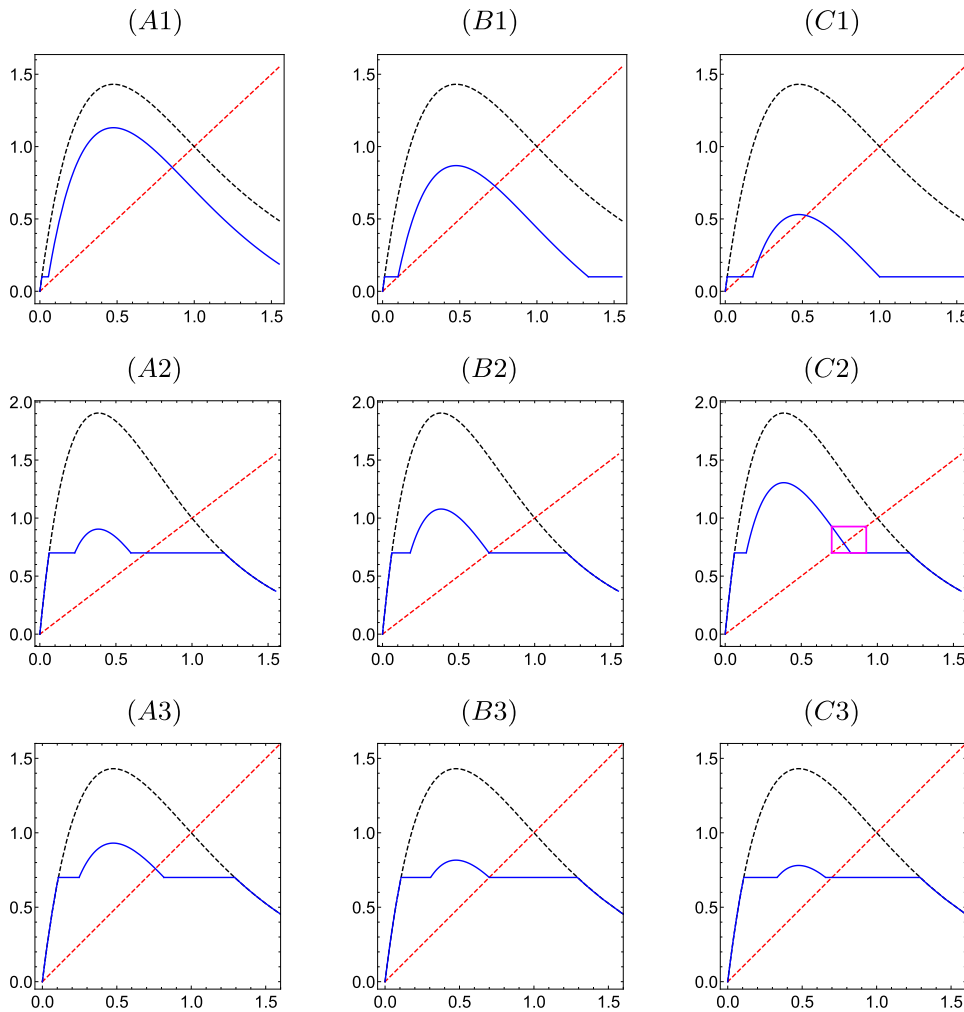


FIG. 5. Illustrations of BCBs arising when $H = f(T) - T$ in (2). The Ricker map $f(x) = xe^{r(1-x)}$ is the black dashed curve, while the blue solid curve is the corresponding map F . The red dashed line is $y = x$. Top panel: fold BCB for $r = 2.1$ and $T = 0.1 < \bar{x} \approx 0.353$. (A1) $H = 0.3 < f(T) - T \approx 0.562$; (B1) $H = f(T) - T$; (C1) $H = 0.9 > f(T) - T$. Center panel: flip BCB for $r = 2.6$ and $T = 0.7 > \bar{x} \approx 0.485$. The attracting 2-cycle is represented by a magenta box in (C2). (A2) $H = 1 > f(T) - T \approx 0.827$; (B2) $H = f(T) - T$; (C2) $H = 0.6 < f(T) - T$. Bottom panel: persistence BCB for $r = 2.1$ and $T = 0.7$ ($\bar{x} < T < \bar{x} \approx 0.77$). (A3) $H = 0.5 < f(T) - T \approx 0.614$; (B3) $H = f(T) - T$; (C3) $H = 0.65 > f(T) - T$.

$H = f(T) - T$, the first three BCBs can occur as T or H are continuously changed. See Fig. 5 for illustrations.

- A fold BCB occurs if $H = f(T) - T$ and $T < \tilde{x}$: T becomes a boundary fixed point as T is decreased or H is increased; after this critical value, two admissible fixed points arise: an attractor T , and a repeller p .
- A flip BCB occurs if $H = f(T) - T$, $T > \tilde{x}$, and q is unstable for g : the attracting fixed point T becomes virtual after becoming a boundary fixed point as T or H decrease, while an unstable fixed point q and an attracting 2-cycle $\{T, g(T)\}$ appear. Notice that the flat shape of F to the right of the break point prevents the possibility of a period-multiplying BCB in our framework.
- A persistence BCB occurs if $H = f(T) - T$, $T \geq \tilde{x}$, and q is asymptotically stable for g : as T or H increase, the virtual fixed point T and the admissible attractor q interchange their roles.

In view of Theorem 7, for a Ricker map $f(x) = x e^{r(1-x)}$, with $r > 2$, a flip BCB occurs when $H = f(T) - T$ and $T > \tilde{x}$, and a persistence BCB occurs when $H = f(T) - T$ and $\tilde{x} \leq T \leq \bar{x}$.

When T becomes a boundary fixed point at the critical value $T = K$, it only makes sense to choose T as the bifurcation parameter; in this case, persistence or flip BCBs can occur as T is continuously changed. These bifurcations are typical of threshold harvesting.^{18,32}

- A persistence BCB occurs if $T = K$ and K is asymptotically stable for f : as T is increased, the fixed point T becomes virtual and the attracting fixed point K becomes admissible.
- A flip BCB occurs if $T = K$ and K is unstable for f : as T is increased, the fixed point T becomes virtual, K becomes admissible, and an attracting 2-cycle $\{T, f(T)\}$ emerges (see Fig. 6).

For the Ricker map, a persistence BCB occurs if $T = 1$ and $0 < r \leq 2$, and a flip BCB occurs if $T = 1$ and $r > 2$.

Finally, smooth local bifurcations of fixed points may also occur for the bifurcation parameter H : a fold SB at $H = f(\tilde{x}) - \tilde{x}$ if $T < \tilde{x}$, and a flip SB when $H = f(\tilde{x}) - \tilde{x}$.

In Figs. 7 and 9, we use solid lines for BCBs of fixed points and dashed lines for SBs of fixed points. Specifically, we use red color for fold bifurcations, orange for persistence BCBs, and brown for flip bifurcations.

BCBs of periodic points and global bifurcations are shown in the case study considered in Subsection V B.

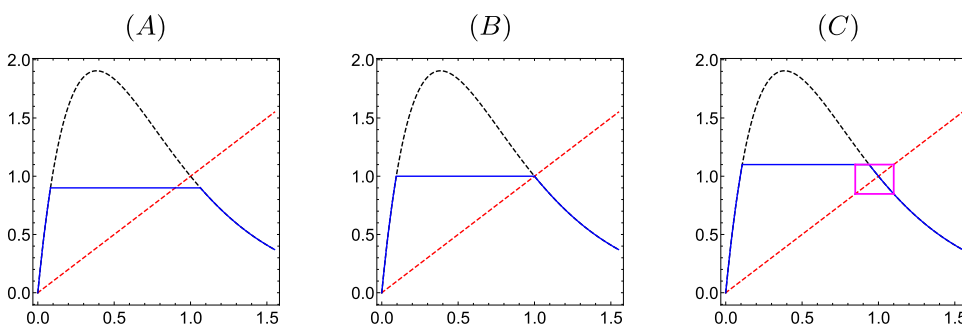


FIG. 6. Illustration of a flip BCB in (2) when $T = K$. The Ricker map $f(x) = x e^{2.6(1-x)}$ is the black dashed curve, while the blue solid curve is the corresponding map F with $H = 1.6$. The red dashed line is $y = x$. The attracting 2-cycle $\{T, f(T)\}$ is represented by a magenta box in panel (c). (a) $T = 0.95 < K = 1$; (b) $T = K$; (c) $T = 1.1 > K$.

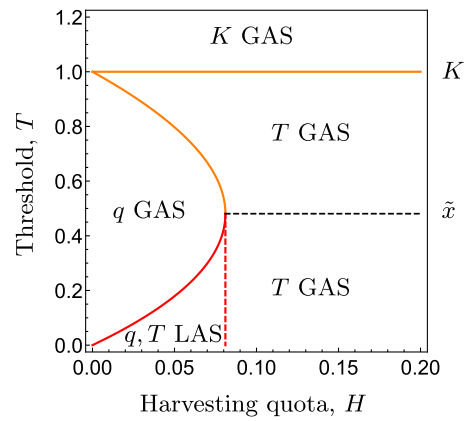


FIG. 7. Stability diagram of PTCH with the Ricker map $f(x) = x e^{0.3(1-x)}$. There is a region of bistability, while in the others there is a unique equilibrium, which is globally attracting. We use orange color for persistence BCBs and red color for fold bifurcations (the solid curve corresponds to a fold BCB, and the dashed line to a fold SB).

IV. ESSENTIAL ATTRACTION AND CHAOTIC BEHAVIOR

In this section, we consider the regions of the parameter plane (H, T) in which complex dynamics is more likely to occur.

First, we consider the case $T < \tilde{x}$ and $H > f(T) - T$. This region of the parameter plane (H, T) is represented in Fig. 9(b) for the Ricker map $f(x) = x e^{2.6(1-x)}$. Shifting the origin of coordinates from $(0, 0)$ to (T, T) , we show that the dynamics of (2) in this case can be derived from the results obtained by Schreiber³⁰ for constant quota harvesting models.

We introduce two definitions for later reference: an equilibrium x^* of a real map $h : I \rightarrow I$ defined on an interval I is *essentially asymptotically stable* if it is stable and $\lim_{n \rightarrow \infty} h^n(x) = x^*$ for Lebesgue almost all x in a neighborhood of x^* . If $\lim_{n \rightarrow \infty} h^n(x) = x^*$ for Lebesgue almost all $x \in I$, we say that x^* is an *essential global attractor*.

A discussion of essential asymptotic stability²² and the relation to Milnor attractors²³ can be found in Ref. 25, where the authors introduce the concept of the stability index.

We state the main result of this subsection:

Theorem 8: Let $f : [0, \infty) \rightarrow [0, \infty)$ be a C^3 unimodal map with negative Schwarzian derivative satisfying (A1) and (A2). If F

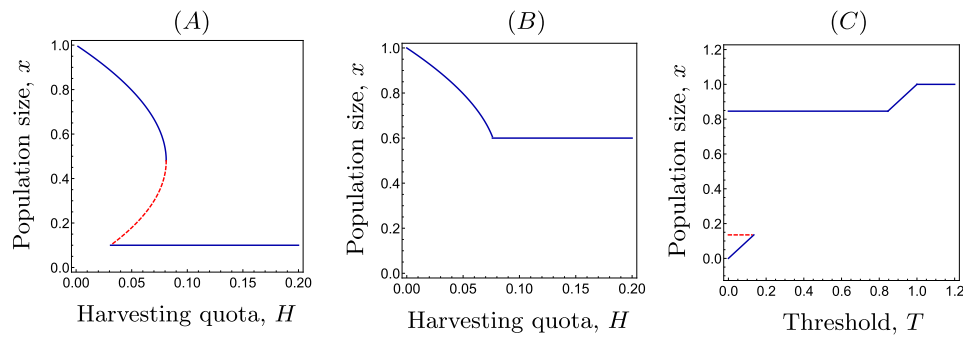


FIG. 8. Bifurcation diagrams for the PTCH model (2) with the Ricker map $f(x) = x e^{0.3(1-x)}$. Red dashed lines correspond to unstable equilibria. (a) $T = 0.1 < \bar{x}$: as harvesting quota is increased, there is a fold BCB and a fold SB; bistability occurs between the two bifurcation points. (b) $T = 0.6 > \bar{x}$: as harvesting quota is increased, there is a persistence BCB. (c) $H = 0.04 < f(\bar{x}) - \bar{x}$: as the threshold is increased, there is a fold BCB and two persistence BCBs. Bistability is observed until the first bifurcation point.

has at least 2 positive fixed points, let

$$p = \min\{x : x > 0, g(x) = x\} \quad \text{and} \quad p^* = \max g^{-1}(p).$$

Assume that $T < \bar{x}$ and $H > f(T) - T$. Then, there are three generic categories for the dynamics of (2),

- (Global attraction) If $H > f(\bar{x}) - \bar{x}$, then T is the only positive fixed point of F , and it is globally asymptotically stable.
- (Bistability) If $H < f(\bar{x}) - \bar{x}$ and $g^2(x_c) > p$, then F has three positive fixed points $T < p < q$. T is asymptotically stable with basin of attraction $(0, p) \cup (p^*, \infty)$ and p is unstable. If $g'(q) \geq -1$, then q is asymptotically stable and attracts (p, p^*) ; hence, every solution of (2) converges to a fixed point. If $g'(q) < -1$, then the interval $[g^2(x_c), g(x_c)]$ is forward invariant, with basin of attraction (p, p^*) .
- (Essential attraction) If $H < f(\bar{x}) - \bar{x}$ and $g^2(x_c) < p$, then F has three positive fixed points and T is an essential global attractor.

Proof. It is clear that the long-term behavior of the solutions of (2) and equation $x_{n+1} = G(x_n)$, $n \geq 0$, is the same, where G was defined in (3). If we shift the origin of coordinates from $(0, 0)$ to (T, T) , then the map G satisfies assumptions (A1)–(A5) in Ref. 30. Thus, the proof follows from Lemma 1 and Theorem 1 in Ref. 30. \square

When H is the bifurcation parameter, the transition from bistability to global attraction of T occurs through a smooth fold bifurcation when p and q collide for $H = f(\bar{x}) - \bar{x}$. For this critical value, F has two positive fixed points T and p ; p is semi-stable with basin of attraction $[p, p^*]$, and T attracts $(0, p) \cup (p^*, \infty)$. In Figs. 7 and 9, the fold bifurcation curve is represented by a red dashed line. The transition between bistability and essential attraction occurs through a boundary collision when $H < f(\bar{x}) - \bar{x}$ and $g^2(x_c) = p$. Schreiber³⁰ calls the dynamics in this case *chaotic semi-stability* because the interval $J = [p, g(x_c)]$ is invariant and F is chaotic on J . Actually, there is a homoclinic orbit containing the critical point x_c (see Ref. 20, Appendix C, for further comments). In Fig. 9(b), we represent the two boundary collisions as H is increased by black dashed lines.

We emphasize that these boundary collisions are not due to the non-smooth character of F ; they occur when the attractor collides with an unstable periodic orbit (a fixed point in this case), and they were introduced by Grebogi *et al.*,¹⁶ who termed them *crises*. Roughly speaking, these bifurcations are able to break chaotic behavior and lead to a simple dynamics in which solutions converge to the equilibrium T with probability one.

We now deal with the case $H < f(T) - T$ (when T is a virtual fixed point), under the same conditions for f . An important issue in this case is the relative position between $g^2(x_c)$ and T . If $g^2(x_c) > T$, then we have two possibilities: (a) if $g(x_c) \leq x_c$ then q is a global attractor, by Lemma 2 and (b) if $g(x_c) > x_c$ then $I = [g^2(x_c), g(x_c)]$ is a forward invariant interval whose basin of attraction is $(0, \infty)$. Hence, the long-term behavior of the solutions of (2) is governed by the map g . If I does not contain any periodic attractor when $g^2(x_c) = T$, then the unique metric attractor of g consists of a finite union of intervals with a dense orbit (Ref. 38, Sec. II.3), and a new form of discontinuity-induced bifurcation occurs at this point, when the metric attractor collides with the break point T . We will refer to this bifurcation as discontinuity-induced crisis. If g has an m -periodic attractor when $g^2(x_c) = T$, then a persistence BCB (for F^m) occurs when this orbit collides with T , that is, when $g^m(T) = T$. In this case, a sequence of period-doubling and period-halving bifurcations giving rise to bubbles³ appear in the bifurcation diagram.

In Subsection V B, we give examples of both situations. The branches of the curve $g^2(x_c) = T$ inside the region $H < f(T) - T$ are represented by green solid lines in Fig. 9.

V. GLOBAL DYNAMICS: CASE STUDIES

A. A compensatory model

We begin with the simple case of compensatory models. In the light of Theorem 7, analogous dynamics is exhibited by the Ricker map if $r \leq 2$.

Here, we consider the Ricker map $f(x) = x e^{r(1-x)}$, with $r = 0.3 < 1$. The corresponding 2-parameter bifurcation diagram follows from Theorems 1 and 2, and it is shown in Fig. 7.

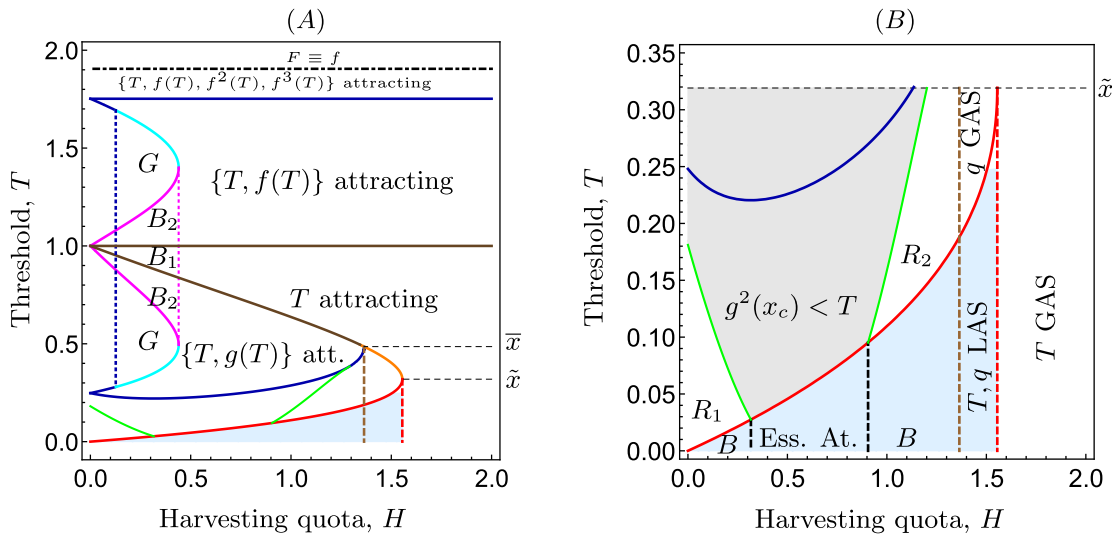


FIG. 9. (a) Main bifurcation boundaries of PTCH with the Ricker map $f(x) = xe^{2.6(1-x)}$. We use solid lines for border-collision bifurcations (BCBs) and dashed or dotted lines for smooth bifurcations (SBs). Bifurcations of fixed points: red for fold BCB, orange for persistence BCB, brown for flip BCB, brown dashed for flip SB, red dashed for fold SB. Bifurcations of 2-cycles: magenta for fold BCB, light blue for persistence BCB, dark blue for flip BCB, blue dotted for flip SB, magenta dotted for fold SB. The dot-dashed black line is defined by $T = f(x_c)$, so $F \equiv f$ for larger values of T . Regions labeled with B_1 and B_2 exhibit bistability, while in regions labeled with G there is a 2-periodic attractor $p_1 \rightarrow g(p_1) = p_2 \rightarrow f(p_2) = p_1$ (see the text). The blue shadowed region and the green lines are explained in (b). (b) Zoom of (A) for $0 < T < \tilde{x}$. According to the results in Subsection IV, when $f(T) - T < H < f(\tilde{x}) - \tilde{x}$ and $T < \tilde{x}$ (blue shadowed region), we find regions of bistability between T and a periodic or chaotic attractor (marked with B); bistability between T and other equilibrium q ; and essential attraction to T . The green lines for $H < f(T) - T$ (where T is not a fixed point) are defined by $g^2(x_c) = T$. Complex behavior may be expected to appear in regions B , R_1 , and R_2 .

There are still some interesting comments. We show in Fig. 8, the three relevant possibilities for bifurcation diagrams as one of the harvesting parameters H, T is changed.

The values of the bifurcation points are easily found. We first compute numerically the value $\tilde{x} \approx 0.4808$ such that $f'(\tilde{x}) = 1$.

For $T = 0.1$, a fold BCB occurs at $H = H_1 = f(T) - T \approx 0.031$ and a fold SB occurs at $H = H_2 = f(\tilde{x}) - \tilde{x} \approx 0.081$. Bistability between H_1 and H_2 induces hysteresis, which can have unexpected consequences for management: assume we increase harvesting quota from a value slightly smaller than H_2 ; then, at $H = H_2$, population falls abruptly to the threshold level $T = 0.1$. Then, we decrease again the quota, but relatively high levels of population abundance might not be recovered until $H < H_1$ [see Fig. 8(a)]. If $T > \tilde{x}$, then there is always a globally stable equilibrium, with a persistence BCB at $H = f(T) - T$; in Fig. 8(b), we show the case $T = 0.6$, with $f(T) - T \approx 0.076$.

When we use T as the bifurcation parameter, the most interesting case occurs when $H < f(\tilde{x}) - \tilde{x}$. For $H = 0.04$ and small T , there are three equilibria: T and the two positive fixed points $p \approx 0.135$ and $q \approx 0.846$ of g . T and q are asymptotically stable, and p is unstable. At the critical value $T = p$, p and T become virtual fixed points through a fold BCB, and q becomes globally attracting until $T = q$, where a persistence BCB occurs and T becomes globally stable. A new persistence BCB occurs at $T = 1$, and, after that, the positive equilibrium $K = 1$ of f is the global attractor [Fig. 8(c)].

B. An overcompensatory model

For overcompensatory models, the dynamics are richer than those exhibited by compensatory maps. In this subsection, we show some interesting phenomena that can be observed in (2) with the Ricker map $f(x) = xe^{r(1-x)}$, $r = 2.6$. For this map, the unharvested population (when $H = 0$) has an attracting 4-cycle. We have chosen this value for r because it has been used by Schreiber³⁰ for constant harvesting, and by Hilker and Liz¹⁸ for threshold harvesting, which can be seen as particular cases of PTCH. In this way, it is easier to relate our results with those in the previous references. Although we expect more complicated dynamics for larger values of r , for which f is chaotic, our case study also shows transitions between order and chaos. As shown by Schreiber³⁰ (see also Ref. 19), maps with a periodic attractor can exhibit chaos when constant harvesting is applied.

We have seen that for compensatory models and for any stable Ricker map, the dynamics of (2) are trivial in the sense that all solutions converge to an equilibrium; in these cases, the BCBs are determined by the pairs (H, T) for which T is a boundary fixed point of F , that is, either $T = K$ or $g(T) = T$ (Fig. 7). For example, in this section, an important role is played by the pairs (H, T) for which T is a boundary fixed point of F^2 . It may also occur that T is a boundary fixed point of F^4 , but for simplicity we restrict our analysis to bifurcations of 2-cycles; we discuss BCBs for F^2 in Subsection V B 1. Other interesting dynamics correspond to the results given in Sec. IV: when $T < \tilde{x}$, boundary collisions can drive the system from a periodic or essential attractor to chaos as H is

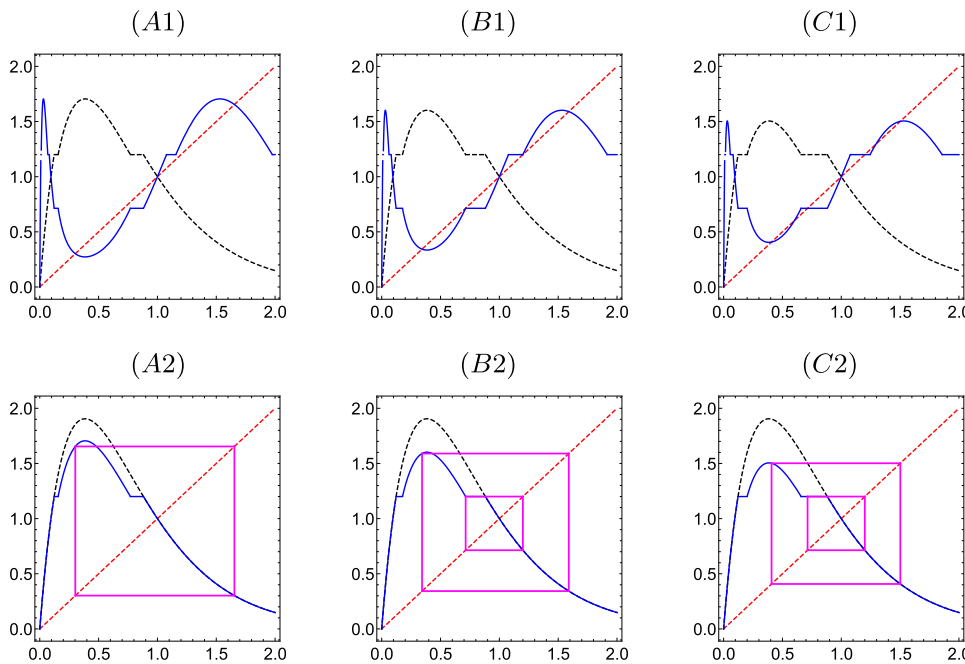


FIG. 10. Illustration of a fold BCB for F^2 in (2) with the Ricker map $f(x) = xe^{2.6(1-x)}$ and $T = 1.2$. The red dashed line is $y = x$. Top panel: the black dashed curve is the graph of F , and the blue solid curve is the graph of F^2 . (A1) $H = 0.2$; (B1) critical value $H = 0.303$, when $F^2(T) = g(f(T)) = T$; (C1) $H = 0.4$. Bottom panel: the black dashed curve is the graph of f , while the blue solid curve is the graph of F . Attracting or semistable 2-cycles of F are represented by magenta boxes. (A2) $H = 0.2$ (one attracting cycle, corresponding to region G in Fig. 9); (B2) $H = 0.303$ (the attracting 2-cycle persists, and a new 2-cycle $\{T, f(T)\}$ arises at the fold BCB and it is semistable; it corresponds to the magenta curve between regions G and B_2 in Fig. 9); (C2) $H = 0.4$ (bistability between two attracting cycles, corresponding to region B_2 in Fig. 9).

increased. Figure 9 shows a 2-parameter bifurcation diagram which describes quite well the dynamics and bifurcations of (2) in terms of the relevant parameters H and T . We also plot in Subsections V B 4 and V B 5 some numerical 1-parameter bifurcation diagrams, which help to understand the main features of the dynamics. We discuss other relevant aspects such as bistability regions and the influence of threshold dynamics in Subsections V B 2 and V B 3, respectively. We emphasize that the bifurcation curves plotted in Fig. 9 have been obtained from analytic expressions (often implicit) and represented using the software Mathematica. The 1-parameter bifurcation diagrams in Figs. 11–14 have been obtained numerically in the usual way: for each value of T or H , a random initial condition is selected from a suitable interval and a number of iterations are plotted, after removing transients.

1. Border-collision bifurcations for F^2

Specific border-collision bifurcations for F^2 are determined by the solutions of $F^2(T) = T$ (with $F(T) \neq T$), so there are four cases:

1. If $T > 1$ and $f^2(T) = T$, then the 2-cycle $\{T, f(T)\}$ becomes attracting as T is decreased for a fixed H , through a flip BCB.
2. If $T > 1$ and $g(f(T)) = T$, then the 2-cycle $\{T, f(T)\}$ emerges or disappear as H or T continuously change in a variety of BCBs (fold, persistence, flip).
3. If $T < 1$ and $f(g(T)) = T$, with $T < g(T)$, then the 2-cycle $\{T, g(T)\}$ emerges or disappear as H or T continuously change in a variety of BCBs (fold, persistence, flip).
4. If $T < 1$ and $g^2(T) = T$, with $T < g(T)$, then the 2-cycle $\{T, g(T)\}$ emerges or disappear as H or T continuously change, through a flip BCB.

In Fig. 9(a), we represent BCBs for F^2 with solid lines: magenta color for fold BCBs, light blue for persistence BCBs, and dark blue for flip BCBs. Figure 10 illustrates a fold BCB corresponding to the second case: as H increases and crosses the magenta bifurcation curve, the virtual cycle $\{T, f(T)\}$ becomes an admissible cycle of F after collision with a virtual fixed point of F^2 (a fixed point of $g \circ f$). After the bifurcation occurs, the cycle $\{T, f(T)\}$ coexists with other admissible attracting 2-cycle (which is destroyed for a larger value of H through a fold smooth bifurcation for F^2).

Remark 1: For $r = 2.6$, the critical value $H_* = H_*(r)$ at which the fold smooth bifurcation for F^2 occurs is $H_* \approx 0.44$, and it is numerically determined as the solution of the nonlinear system $f(g(x)) = x, f'(g(x))g'(x) = 1$. See the magenta dotted line in Fig. 9(a). The graph of the function $r \rightarrow H_*(r)$ can be plotted numerically, and it is an increasing function of r , with $H_*(2^+) = 0$. Recall that, by Theorem 7, F does not have other 2-cycles than the fixed points if $r \leq 2$. We conjecture that T is a global attractor for (2) with the Ricker map if (H, T) belongs to the region

$$R = \{(H, T) : H > H_*(r), H \geq f(T) - T, x_c < T < 1\}.$$

This would complete the global stability region shown in Fig. 4. The reason why we think the conjecture is true is that F is a continuous map and, once the 2-cycle is destroyed in the fold bifurcation, no other 2-cycles seem to appear. Hence, due to Coppel’s results,⁷ T is a global attractor.

2. Bistability regions

An important consequence of fold bifurcations (either smooth or border-collision) is that they create or destroy regions of bistability. Bistability has important consequences in population dynamics

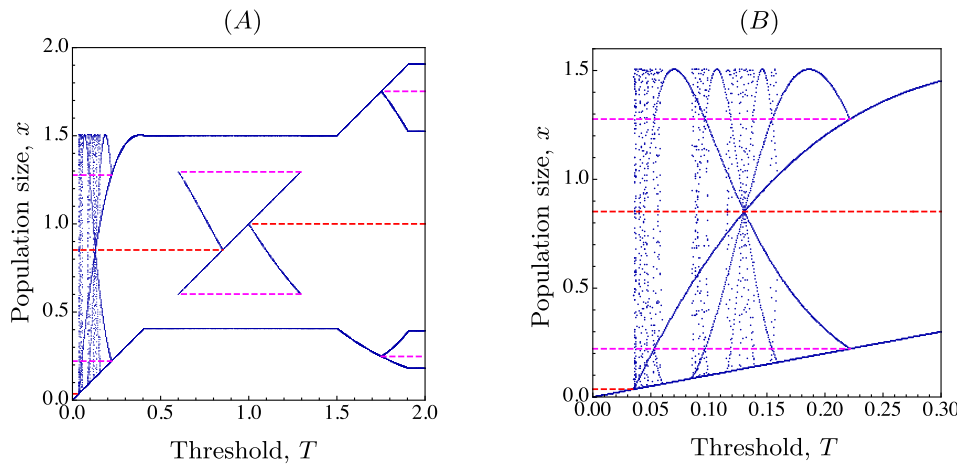


FIG. 11. (a) Bifurcation diagram for (2) with the Ricker map $f(x) = x e^{2.6(1-x)}$, $H = 0.4$, and bifurcation parameter $T \in (0, 2)$. (b) Zoom of (a) for $0 < T < 0.3$. Red dashed lines represent unstable fixed points of F ($\rho < q < K = 1$), and magenta dashed lines denote unstable 2-cycles of F .

because in this case the long-term behavior of the solutions strongly depends on the initial condition.

As H or T are continuously changed, regions of bistability in the 2-parameter diagram shown in Fig. 9 appear between two fold bifurcation curves, with the only exception of a region of essential attraction. For small values of T , we find these regions between the curve $H = f(T) - T$ and the vertical line $H = f(\bar{x}) - \bar{x}$. The regions marked with B represent bistability between the attracting equilibrium T and a periodic or chaotic attractor, and there is a region where two attracting fixed points coexist. In the region of essential attraction, solutions converge to T with probability one, so there is not bistability. This dynamical behavior has already been observed for models of constant quota harvesting,^{20,30} and it is explained in Sec. IV.

For larger values of T , we find a region of bistability between fold bifurcation branches for F^2 . We distinguish two types of regions labeled with B_1 and B_2 in Fig. 9(a). In region B_1 , the equilibrium T is attracting, and it coexists with another periodic attractor \mathcal{A} , with period 2 or 4. In region B_2 , the attracting 2-cycle $\{T, f(T)\}$ (if $T > 1$) or $\{T, g(T)\}$ (if $T < 1$) coexists with the attractor \mathcal{A} . The

period of \mathcal{A} is 4 if $H < H^* \approx 0.126$ and 2 if $H \geq H^*$, where H^* can be numerically approximated solving the nonlinear system $f(g(x)) = x$, $f'(g(x))g'(x) = -1$. The (smooth) period-doubling bifurcation at $H = H^*$ is represented by the vertical blue dotted line in Fig. 9(a).

3. The influence of threshold dynamics

In Fig. 9, we can identify large regions where the dynamics of (2) is governed by the flat part of F . In this situation, we do not expect complicated dynamics, since, with probability one, all orbits fall into a stable periodic attractor of the form $\{T, F(T), \dots, F^m(T)\}$. The period m is the return period of the orbit to the flat part, starting at T . In the case of threshold harvesting (TH), m can be determined as the least positive integer for which $f^m(T) \geq T$.³² In the same reference, we can find typical features of the bifurcation diagram for flat-topped maps that are also present in the dynamics of PTCH. For example, ranges of effectively chaotic behavior (corresponding to periodic orbits of long period), chaotic windows, and “star-like” intersections in the bifurcation diagram.

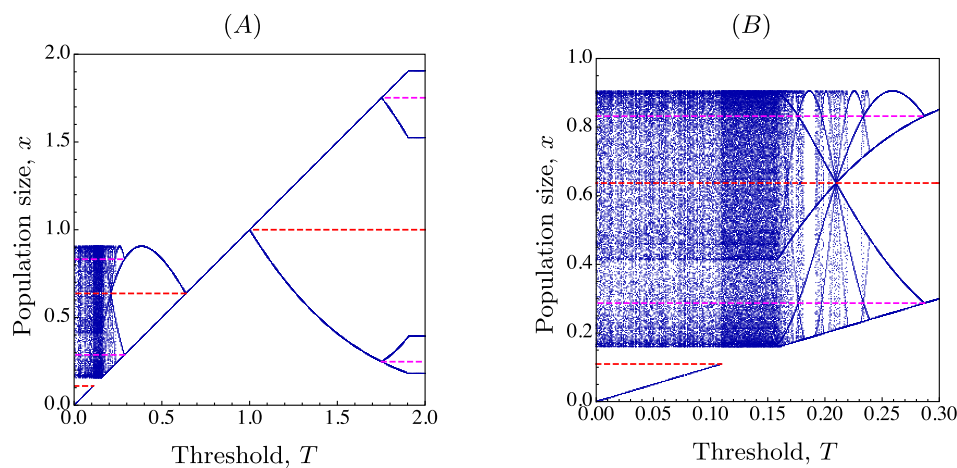


FIG. 12. (a) Bifurcation diagram for (2) with the Ricker map $f(x) = x e^{2.6(1-x)}$, $H = 1$, and bifurcation parameter $T \in (0, 2)$. (b) Zoom of (A) for $0 < T < 0.3$. Red dashed lines represent unstable fixed points of F ($\rho < q < 1$), and magenta dashed lines correspond to unstable 2-cycles.

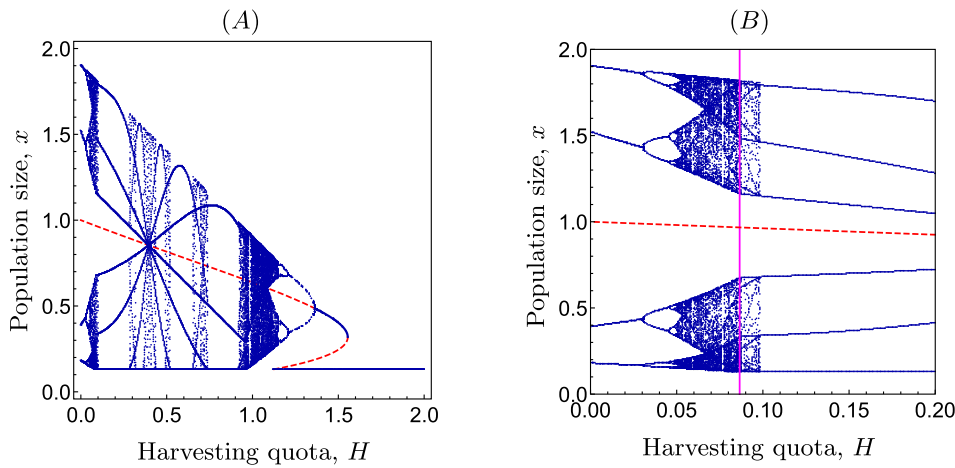


FIG. 13. (a) Bifurcation diagram for (2) with the Ricker map $f(x) = x e^{2.6(1-x)}$, $T = 0.13$, and bifurcation parameter $H \in (0, 2)$. (b) Zoom of (A) for $0 < H < 0.2$. Red dashed lines represent unstable fixed points of F ($p < q < 1$), and the magenta vertical line denotes a discontinuity-induced crisis (see the text).

The simplest case occurs when m is a power of 2: in this case, decreasing T leads to a sequence of period-halving bifurcations until T becomes a global attractor for $T \leq K$.¹⁸ We observe this bifurcation scenario when $H + T \geq f(x_c)$, corresponding to the rightmost region in Fig. 9(a) (in this case, PTCH becomes TH).

There are other parameters for which the orbit of T converges to an attractor that does not contain T . In these cases, it is possible that a single periodic orbit governs the long-term behavior of almost all solutions, as in regions marked with G in Fig. 9(a) [see, e.g., Fig. 10(A2)], but the attractor can also be chaotic. This complicated behavior can be expected for some values of (H, T) in regions marked with B, R_1 , and R_2 in Fig. 9(b). Increasing T tends to prevent chaotic behavior, but increasing H can either induce or prevent chaos, as it happens in a strategy of constant quota harvesting (see, e.g., Ref. 30, Fig. 3).

4. Case studies when T is the bifurcation parameter

In this subsection, we choose two particular values of the maximum allowed harvesting quota H and study the changes in the

dynamics of (2) as the threshold harvesting T is increased, that is, as the harvest rule PTCH becomes more conservative. As we can see in Fig. 9(a), for sufficiently large values of H , there is a unique attractor, which is the periodic orbit of T (1, 2, or 4-periodic). For small values of H , in particular, for $H < H_* \approx 0.44$ (see Remark 1), the dynamics is more influenced by BCBs for F^2 . We plot the bifurcation diagrams in two cases: $H = 0.4 < H_*$ and $H = 1 > H_*$.

We begin with $H = 0.4$. Since g does not depend on T , the fixed points of g are virtual or admissible fixed points of F for every T . We obtain numerically that $p \approx 0.035 < q \approx 0.852$. Since $g'(p) > 1$ and $g'(q) < -1$, both are unstable.

As T ranges from 0 to 2, there are ten border-collision bifurcations (see Fig. 11). For small values of T , a zoom of the bifurcation diagram shows the first one, which occurs for $T = T_1 = p \approx 0.035$, in a fold BCB: the admissible fixed point T is an essential attractor for $T < T_1$; then it becomes virtual and a periodic attractor containing T arises. Between T_1 and $T_2 \approx 0.2216$, we can observe typical features of bifurcation diagrams for piecewise smooth maps with flat branches: intervals of effective chaotic behavior (periodic attractors with long periods) alternate with periodic windows and star-like

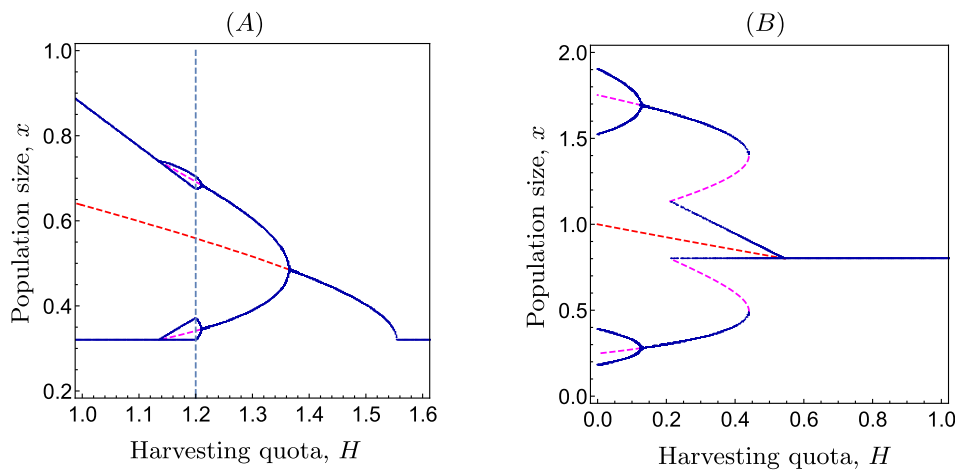


FIG. 14. Bifurcation diagrams for (2) with the Ricker map $f(x) = x e^{2.6(1-x)}$ and bifurcation parameter H . (a) $T = \tilde{x} \approx 0.32$ and $H \in (1, 1.6)$; (b) $T = 0.8$ and $H \in (0, 1)$. In both cases, the red dashed line represents the unstable fixed point q of g , and magenta dashed lines correspond to unstable 2-cycles. The dashed vertical line in (A) denotes a persistence BCB for F^4 , giving rise to a bubble (see the text).

structures.³² For example, we can see a star for $T \approx 0.13$, when $g(T) = q$. At $T = T_2$ [satisfying $g^2(T_2) = T_2$], there is a flip BCB, and $\{T, g(T)\}$ becomes an attracting 2-cycle. After a persistence BCB at $T = T_3 \approx 0.407$ [where $f(g(T_3)) = T_3$], $\{T, g(T)\}$ is replaced by a 2-periodic orbit $\{p_1, p_2\}$, with $f(g(p_1)) = p_2$. There is bistability for $T \in (T_4, T_7)$, where $T_4 \approx 0.602$ and $T_7 \approx 1.294$ correspond to fold BCBs of F^2 ; in particular, the fixed point T coexists with $\{p_1, p_2\}$ in (T_5, T_6) , where $T_5 \approx 0.852$ and $T_6 = 1$ correspond to flip BCBs. At $T_8 \approx 1.5$, the 2-cycle $\{T, f(T)\}$ becomes attracting after a persistence BCB; this cycle becomes unstable at $T_9 \approx 1.75$, in a flip BCB, after which $\{T, f(T), f^2(T), f^3(T)\}$ becomes attracting. Finally, this 4-cycle is replaced by the attracting 4-cycle of f at $T_{10} \approx 1.9$.

Next, we consider $H = 1$, which exhibits some new features; the corresponding bifurcation diagram is shown in Fig. 12. The fixed points of g are now $p \approx 0.109 < q \approx 0.637$, and they are unstable. Since $H > H_*$, bistability is not observed for intermediate values of T . However, for small values of T , bistability occurs between the equilibrium T and a chaotic attractor of g . Bistability is observed for $T < p$; at $T = p$, the admissible fixed point T becomes virtual after a fold bifurcation. The chaotic attractor persists for $T \in (p, T^*)$, where $T^* \approx 0.158$ corresponds to a discontinuity-induced crisis, when the lower edge of the chaotic interval collides with T ($g^2(x_c) = T^*$); this bifurcation changes abruptly the dynamics, from a chaotic attractor to a periodic attractor defined by the superstable orbit of T . After that, typical behavior of maps with flat intervals occur, as explained in the previous case. Notice that the equilibrium T is globally asymptotically stable for $T \in (q, 1)$ (see Theorem 3 and Fig. 4); a sequence of two flip BCBs (period-halving and period-doubling) occurs as T increases and collides with q and 1, respectively. For $T > q$, the bifurcation diagram coincides with the bifurcation diagram of TH (compare with Ref. 18, Fig. 3).

5. Case studies when H is the bifurcation parameter

As we have already mentioned, for $T = 0$ PTCH becomes the constant quota harvesting strategy defined by the map $F(x) = \max\{f(x) - H, 0\}$. For the Ricker map $f(x) = x e^{r(1-x)}$, the dynamics of F depending on r and H was studied by Schreiber.³⁰ In particular, the bifurcation diagram for $r = 2.6$ corresponds to Fig. 5(b) in that reference, and it is characterized by two intervals of bistability (where zero and an interval bounded away from zero are attracting), an interval of essential extinction, and total extinction for large values of H due to overharvesting. As explained in Sec. IV, for small values of $T > 0$, for which T is an admissible fixed point, a similar situation holds for (2), but extinction is not possible due to the positive minimum biomass level T . In this subsection, we consider three different values of T and plot the corresponding bifurcation diagrams as H increases; as expected, larger values of T not only help to avoid extinction but also tend to simplify the dynamics.

Recall that there is a point $\tilde{x} \approx 0.32$ such that $f'(\tilde{x}) = 1$. If $T < \tilde{x}$, then a fold SB occurs at $H = \tilde{H} := f(\tilde{x}) - \tilde{x} \approx 1.555$, and T is a global attractor for $H > \tilde{H}$.

We begin with $T = 0.13 < \tilde{x}$. As H is increased from zero, the curve defined by $g^2(x_c) = T$ is crossed twice [see Fig. 9(b)]. Looking at the 2-parameter bifurcation diagram in that figure, the dynamics starts in region R_1 , where the 4-periodic attractor of g for $H = 0$

undergoes a route of period-doubling bifurcations to chaos. After a first discontinuity-induced crisis at $H = H_1 \approx 0.086$ [magenta vertical line in Fig. 13(b)], the dynamics is governed by the superstable periodic orbit of T . Notice that there are still periodic orbits with long periods until a 6-periodic window appears at $H \approx 0.098$, when $g^6(T) = T$; see Ref. 32, p. 4836, for comments on periodic windows.

Then we observe, as in the previous examples, a typical bifurcation diagram of maps with flat segments for $H \in (H_1, H_2)$ [see, for example, the star-like structure at $H \approx 0.394$, for which $g(T)$ is a fixed point of g], where at $H_2 \approx 0.959$ the second discontinuity-induced crisis occurs. We notice that at the first crisis, the metric attractor of g consists of two intervals, while in the second one, it consists of only one interval; in both cases the bifurcation occurs when T collides with the smallest point of the attractor, that is, when $g^2(x_c) = T$. The dynamics is again chaotic in region R_2 , until a series of period-halving bifurcations leads to an attracting fixed point at $H_4 \approx 1.364$. At $H_3 \approx 1.118$, T becomes an admissible fixed point in a fold BCB. There is bistability for $H \in (H_3, H_5)$, where $H_5 = \tilde{H}$.

For $T \geq \tilde{x}$, Eq. (2) does not exhibit complex behavior. In Fig. 14, we show the bifurcation diagram in two particular cases: $T = \tilde{x}$ and $T = 0.8 > \tilde{x}$. When $T = \tilde{x}$, we show the bifurcation diagram for $H \in (1, 1.6)$, where we underline two interesting features:

- first, the period-doubling bifurcation cascade observed in Fig. 13 as H is reduced from $H = \tilde{H}$ is broken in this case when the attracting 4-periodic cycle of g collides with the superstable 4-periodic orbit $\{T, g(T), g^2(T), g^3(T)\}$ at $H \approx 1.2$ [persistence BCB for F^4 , represented by a vertical dashed line in Fig. 14(a)]. Thus, the sequence of flip bifurcations to chaos is replaced by a bubble in the bifurcation diagram and
- second, the fold SB that occurs at $H = \tilde{H}$ when $T < \tilde{x}$ does not take place in this case; instead, we observe a persistence BCB, since $g(T) = g(\tilde{x}) = \tilde{x} = T$.

When $T = 0.8$, we distinguish four bifurcations as H ranges from 0 to 1. For $H < H_1 = H^* \approx 0.126$, there is an attracting 4-periodic cycle of F ; at $H = H_1$, a flip SB leads to an attracting 2-cycle of F . At $H = H_2 \approx 0.211$, a fold BCB occurs when $f(g(T)) = T$, and $\{T, g(T)\}$ becomes attracting. Both attracting 2-cycles coexist until the first one disappears at $H = H_3 = H_* \approx 0.44$ in a fold SB for F^2 . The segment (H_1, H_2) corresponds to region G in Fig. 9(a), and (H_2, H_3) to region B_2 . Finally, the 2-cycle $\{T, g(T)\}$ is destroyed in a flip BCB at $H = H_4 = f(T) - T \approx 0.545$, and T becomes an attractor for $H \geq H_4$.

VI. DISCUSSION

Piecewise smooth dynamical systems are undergoing an increasing interest for two main reasons: on the one hand, they find applications in various fields, like economics, social sciences, electronics, mechanics, population management, and control, among others;^{1,2,28,31,37} on the other hand, they exhibit a rich dynamics, including new bifurcations different from the well known bifurcations for smooth maps. In this paper, we present a new example of piecewise map that comes from a precautionary threshold constant-catch harvesting strategy (PTCH). An important characteristic of this map is that it has flat branches, which in some cases lead to superstable attractors. In this situation, border-collision bifurcations

play an essential role. Piecewise smooth maps with flat branches appear in different applications, ranging from chaos control^{8,15,32,36} to economic models,^{1,5,37} and sustainable harvest rules.¹⁸

PTCH can be seen as a combination of constant catch harvesting (CH for short) and threshold harvesting (TH) rules. The maps governing these two strategies are piecewise smooth: the graph of the map for constant harvesting has a flat part at the bottom,³⁰ and the corresponding map for TH is flat-topped.¹⁸ The dynamics of PTCH is strongly influenced by both maps: results valid for CH help understanding the dynamics of PTCH for small values of T , and typical features of the bifurcation diagrams of TH are present in those of PTCH. As a result, the dynamics of PTCH is richer than and qualitatively different from the dynamics of TH and other threshold rules as proportional threshold harvesting (PTH, for short) (see, e.g., Ref. 17).

We combine analytical and numerical results to provide a comprehensive overview of the dynamics of PTCH. For simple cases (compensatory models), the dynamics and bifurcations are thoroughly described analytically. As expected, overcompensatory models exhibit more complicated dynamics; in this case, some regions of the 2-parameter plane (H, T) can be completely understood; for example, some global stability results (Subsection III B 2), and regions where bistability or essential attraction occur (Sec. IV). We have chosen as case study a Ricker model which in the absence of harvesting is oscillatory but not chaotic. This choice allows us to provide good 2-parameter bifurcation diagrams (Fig. 9) and also to compare our results with those obtained for CH by Schreiber³⁰ and for TH by Hilker and Liz.¹⁸ Selected numerical bifurcation diagrams illustrate the main dynamical features of PTCH, which include bistability regions created and destroyed by fold bifurcations or boundary collisions, sudden transitions between chaos and periodic attractors, and bubbles, among others.

From a biological point of view, PTCH is a harvesting rule that helps preventing some undesirable consequences of traditional harvesting strategies, and, in particular, of constant quota harvesting, which can lead to sudden collapses due to overexploitation. The main drawback of a threshold approach is the fisheries moratoria associated with low stock size. A combined strategy like PTCH also helps to overcome this weakness of threshold harvesting rules. In this direction, a manager would be interested in situations where the long-term dynamics is governed either by g (usual constant harvesting) or by g and the threshold T . The reason is that periods without harvesting only appear when f plays a role in the definition of F . As it is expected, this undesirable situation corresponds to a combination of high values of T and small values of H (more conservative strategies).

In contrast with other threshold harvesting rules (TH, PTH), the fixed point of F does not need to be unique for the usual unimodal maps. When two stable equilibria coexist, we observe a phenomenon similar to the so-called Allee effect: too low or too high population densities asymptotically approach the threshold value T , while intermediate population densities tend to a higher equilibrium.

There are two different forms of increasing harvesting effort in PTCH: increasing the harvesting quota H or decreasing the threshold value T . For large H , PTCH becomes TH, and, therefore, a stable equilibrium cannot be destabilized increasing harvesting by

decreasing the threshold.¹⁸ However, fixing a lower value of H , decreasing T can produce several stability switches, some of them destabilizing. For the Ricker map, increasing H cannot destabilize a stable equilibrium. However, it might occur for other population models governed by unimodal maps with negative Schwarzian derivative. Examples of such situations for a strategy of constant quota harvesting are provided by Jiménez López and Liz.¹⁹

ACKNOWLEDGMENTS

The authors thank Professor F. M. Hilker and two anonymous reviewers for their constructive and useful comments and for pointing out some references. Eduardo Liz acknowledges the support of the Research Grant No. MTM2017-85054-C2-1-P (AEI/FEDER, UE). The research of Cristina Lois-Prados has been partially supported by the Ph.D. Scholarship No. FPU18/00719 (Ministerio de Ciencia, Innovación y Universidades, Spain) and Research Grant Nos. MTM2016-75140-P (AEI/FEDER, UE) and ED431C2019/02 (Xunta de Galicia).

APPENDIX A: PROOFS

1. Proof of Theorem 2

The proof of Theorem 2 in the main text follows the proof of the analogous result for proportional threshold harvesting (Ref. 17, Proposition A.3). It is an easy application of the following lemma:

Lemma A.3: (Ref. 11, Theorem B) Assume that $f: (0, \infty) \rightarrow (0, \infty)$ has a globally attracting equilibrium K , and let $h: (0, \infty) \rightarrow (0, \infty)$ be a continuous map satisfying that $x < h(x) \leq \max\{f(x), K\}$ for all $x < K$ and $x > h(x) \geq \min\{f(x), K\}$ for all $x > K$. Then, K is a globally attracting equilibrium of h .

Proof. To prove the theorem, let us show that the conditions of Lemma 3 are fulfilled with $h = F$. First, by Proposition 1, K is the unique positive equilibrium of (2). In particular, $x < F(x)$ for all $x < K$. Hence, the result is trivial for $x < K$ because $F(x) \leq f(x) \leq \max\{f(x), K\}$ for all $x \geq 0$. Now, it is clear by (2) that $F(x) \geq \min\{f(x), T\}$, and therefore, since we are assuming that $T \geq K$, it follows that $x > F(x) \geq \min\{f(x), T\} \geq \min\{f(x), K\}$ for all $x > K$. \square

2. Proof of Theorems 5 and 6

Proof of Theorem 5. To prove (i) when $f(T) - T \leq H < f(\tilde{x}) - \tilde{x}$, notice that g has negative Schwarzian derivative and by Proposition 2, $g'(q) \geq -1$. Hence, q is a local attractor of g and we can define J as the connected component of the set $S = \{x \in (p, p^*) : \lim_{n \rightarrow \infty} g^n(x) = q\}$ containing q . Clearly, $J = (a, b)$ is an open interval. If $J \neq (p, p^*)$, then, since g has no other fixed point than q in J , the only possibility is that $g(a) = b$ and $g(b) = a$. But this case is ruled out by Singer's results (see, e.g., Ref. 34, Lemma 2.6). Finally, it is obvious that T attracts $[0, \infty) \setminus [p, p^*]$ if $T < p$ and attracts $[0, \infty) \setminus (p, p^*)$ if $T = p$. The case $H = f(\tilde{x}) - \tilde{x}$ is left to the reader.

To prove (ii), we use a different approach, following the ideas used in Ref. 17, Proposition A.4. Let us consider $T \in (0, 1)$, $H \in (0, f(T) - T)$ arbitrarily fixed; we prove that q is a global attractor using the enveloping method (Ref. 9, Theorem 3). For that purpose, we consider the linear map $\phi(x) = 2q - x$ and show that F

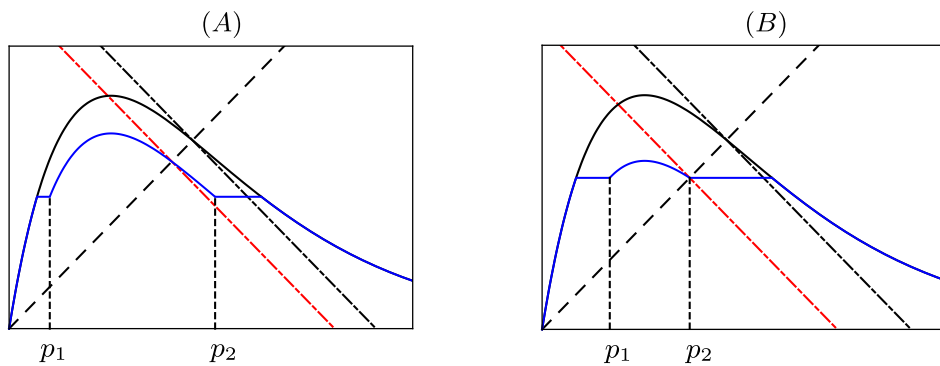


FIG. 15. Diagrams showing the map F (blue solid curve) enveloped by ϕ (red dot-dashed line). The original Richer map $f(x) = xe^{1.8(1-x)}$ is represented by the solid black curve, which is enveloped by the black dot-dashed line $y = 2 - x$. The black dashed line is $y = x$. (a) $\phi(x) = 2q - x$. The equilibrium q is GAS for $T \in (0, 1)$ and $H \in (0, f(T) - T)$. (b) $\phi(x) = 2T - x$. The equilibrium T is GAS for $T \in (x_c, 1)$ and $H \geq f(T) - T$.

fulfills the following inequalities: $x < F(x) < \phi(x)$ for all $x \in (0, q)$, and $x > F(x) > \phi(x)$ for all $x > q$ [see Fig. 15(a)].

We know by Proposition 1 that q is the unique fixed point of F in $(0, \infty)$; moreover, $x < F(x)$ for all $x \in (0, q)$ and $x > F(x)$ for all $x > q$. Hence, it remains to prove that $F(x) < 2q - x$ for all $x \in (0, q)$ and $F(x) > 2q - x$ for all $x > q$.

Let us consider p_1 and p_2 the points such that

$$0 < p_1 < T < q < p_2, \quad g(p_1) = T = g(p_2).$$

Note that, for all $x \in (p_1, p_2)$, we have $F(x) = g(x)$, so F is differentiable in (p_1, p_2) . We distinguish three cases:

- If $x \in (0, p_1]$, then $F(x) = \min\{f(x), T\} \leq T < 2T - x < 2q - x$.
- If $x \in (p_1, p_2)$, then $F(x) = g(x)$. By Proposition 2, $g'(x) \geq -1$ for all $x > 0$; moreover, $g'(x) > -1$ for all $x \neq 1$. Hence, the mean value theorem guarantees that $g(x) \neq 2q - x$ for all $x \neq q$. Therefore, $g(x) < 2q - x$ for all $x \in (p_1, q)$ and $g(x) > 2q - x$ for all $x \in (q, \infty)$.
- If $x > p_2$, then we have $F(x) > g(x) > 2q - x$.

An application of Cull's theorem proves that q is globally asymptotically stable. \square

The proof of Theorem 6 follows from analogous arguments to those used in the proof of Theorem 5, using the line $\phi(x) = 2T - x$ for enveloping, instead of $2q - x$ [see Fig. 15(b)].

DATA AVAILABILITY

The data that support the findings of this study are available from the corresponding author upon reasonable request.

REFERENCES

- 1A. Agliari, P. Commendatore, I. Foroni, and I. Kubin, "Border collision bifurcations in a footloose capital model with first nature firms," *Comput. Econ.* **38**, 349–366 (2011).
- 2M. di Bernardo and P. Kowalczyk, *Piecewise-smooth Dynamical Systems: Theory and Applications*, Applied Mathematical Sciences Vol. 163 (Springer-Verlag, London, 2008).
- 3M. Bier and T. C. Bountis, "Remerging Feigenbaum trees in dynamical systems," *Phys. Lett. A* **104**, 239–244 (1984).
- 4E. Braverman and E. Liz, "Global stabilization of periodic orbits using a proportional feedback control with pulses," *Nonlinear Dyn.* **67**, 2467–2475 (2012).
- 5S. Brianzoni, E. Michetti, and I. Sushko, "Border collision bifurcations of superstable cycles in a one-dimensional piecewise smooth map," *Math. Comput. Simul.* **81**, 52–61 (2010).

- 6D. S. Butterworth, "A suggested amendment to the harvesting strategy used at ICSEAF to specify hake TAC levels," *Colln. Sci. Pap. Int. Commn. S.E. Atl. Fish.* **14**, 101–108 (1987).
- 7W. A. Coppel, "The solution of equations by iteration," *Proc. Camb. Philos. Soc.* **51**, 41–43 (1955).
- 8N. J. Corron, S. D. Pethel, and B. A. Hopper, "Controlling chaos with simple limiters," *Phys. Rev. Lett.* **84**, 3835–3838 (2000).
- 9P. Cull, "Population models: Stability in one dimension," *Bull. Math. Biol.* **69**, 989–1017 (2007).
- 10J. J. Deroba and J. R. Bence, "A review of harvest policies: Understanding relative performance of control rules," *Fish. Res.* **94**, 201–233 (2008).
- 11H. A. El-Morshey and V. Jiménez López, "Global attractors for difference equations dominated by one-dimensional maps," *J. Differ. Equ. Appl.* **14**, 391–410 (2008).
- 12K. Enberg, "Benefits of threshold strategies and age-selective harvesting in a fluctuating fish stock of Norwegian spring spawning herring *Clupea harengus*," *Mar. Ecol. Prog. Ser.* **298**, 277–286 (2005).
- 13S. Engen, R. Lande, and B. E. Sæther, "Harvesting strategies for fluctuating populations based upon uncertain population estimates," *J. Theor. Biol.* **186**, 201–212 (1997).
- 14D. Franco, J. Perán, and J. Segura, "Stability for one-dimensional discrete dynamical systems revisited," *Discrete Contin. Dyn. Syst. B* **25**, 635–650 (2020).
- 15L. Glass and W. Zeng, "Bifurcations in flat-topped maps and the control of cardiac chaos," *Int. J. Bifurcat. Chaos Appl. Sci. Eng.* **4**, 1061–1067 (1994).
- 16C. Grebogi, E. Ott, and J. A. Yorke, "Chaotic attractors in crisis," *Phys. Rev. Lett.* **48**, 1507–1510 (1982).
- 17F. M. Hilker and E. Liz, "Proportional threshold harvesting in discrete-time population models," *J. Math. Biol.* **79**, 1927–1951 (2019).
- 18F. M. Hilker and E. Liz, "Threshold harvesting as a conservation or exploitation strategy in population management," *Theor. Ecol.* (published online, 2020).
- 19V. Jiménez López and E. Liz, "Destabilization and chaos induced by harvesting: Insights from one-dimensional discrete-time models," *J. Math. Biol.* (submitted).
- 20E. Liz, "Complex dynamics of survival and extinction in simple population models with harvesting," *Theor. Ecol.* **3**, 209–221 (2010).
- 21E. Liz and D. Franco, "Global stabilization of fixed points using predictive control," *Chaos* **20**, 023124 (2010).
- 22I. Melbourne, "An example of a nonasymptotically stable attractor," *Nonlinearity* **4**, 835–844 (1991).
- 23J. Milnor, "On the concept of attractor," *Commun. Math. Phys.* **99**, 177–195 (1985).
- 24H. E. Nusse and J. A. Yorke, "Border-collision bifurcations including 'period two to period three' for piecewise smooth systems," *Physica D* **57**, 39–57 (1992).
- 25O. Podvigina and P. Ashwin, "On local attraction properties and a stability index for heteroclinic connections," *Nonlinearity* **24**, 887–929 (2011).
- 26A. E. Punt, "Harvest control rules and fisheries management," in *Handbook of Marine Fisheries Conservation and Management*, edited by R. Q. Grafton, R.

Hilborn, D. Squires, M. Tait, and M. J. Williams (Oxford University Press, 2010), Chap. 44, pp. 582–594.

²⁷T. J. Quinn and R. B. Deriso, *Quantitative Fish Dynamics* (Oxford University Press, New York, 1999).

²⁸D. Radi and L. Gardini, “A piecewise smooth model of evolutionary game for residential mobility and segregation,” *Chaos* **28**, 055912 (2018).

²⁹W. E. Ricker, “Stock and recruitment,” *J. Fish. Res. Board Can.* **11**, 559–623 (1954).

³⁰S. Schreiber, “Chaos and population disappearances in simple ecological models,” *J. Math. Biol.* **42**, 239–260 (2001).

³¹J. Segura, F. M. Hilker, and D. Franco, “Degenerate period adding bifurcation structure of 1D bimodal piecewise linear maps,” *SIAM J. Appl. Math.* **80**, 1356–1376 (2020).

³²S. Sinha, “Unidirectional adaptive dynamics,” *Phys. Rev. E* **49**, 4832–4842 (1994).

³³S. Sinha, “Using thresholding at varying intervals to obtain different temporal patterns,” *Phys. Rev. E* **63**, 036212 (2001).

³⁴D. Singer, “Stable orbits and bifurcation of maps of the interval,” *SIAM J. Appl. Math.* **35**, 260–267 (1978).

³⁵E. M. Steiner, K. R. Criddle, and M. D. Adkison, “Balancing biological sustainability with the economic needs of Alaska’s sockeye salmon fisheries,” *N. Am. J. Fish. Manage.* **31**, 431–444 (2011).

³⁶R. Stoop and C. Wagner, “Scaling properties of simple limiter control,” *Phys. Rev. Lett.* **90**, 154101 (2003).

³⁷I. Sushko, L. Gardini, and K. Matsuyama, “Superstable credit cycles and U-sequence,” *Chaos Soliton Fract.* **59**, 13–27 (2014).

³⁸H. Thunberg, “Periodicity versus chaos in one-dimensional dynamics,” *SIAM Rev.* **43**, 3–30 (2001).

³⁹C. T. Zhou, “Stabilizing long-period orbits via symbolic dynamics in simple limiter controllers,” *Chaos* **16**, 013109 (2006).